TITLE: Wnt/β-catenin signalling assists cell fate decision making in the early mouse embryo

Running title: Wnt/β-catenin signalling in mouse embryo

Names and affiliations of authors: Joaquin Lilao-Garzón[1,2,3], Elena Corujo-Simon[1,4], Meritxell Vinyoles[5,6], Sabine C. Fischer[7], José Guillén[2], Tina Balayo[2,8], and Silvia Muñoz-Descalzo[1,2,*]

1: Department of Biology & Biochemistry, University of Bath, Claverton Down, Bath BA2 7AY, UK.

2: Instituto Universitario de Investigaciones Biomédicas y Sanitarias (IUIBS), Universidad de las Palmas de Gran Canaria (ULPGC), Paseo Blas Cabrera Felipe "Físico" 17, Las Palmas 35016, Spain.

3: Present address: Janelia Research Campus, Howard Hughes Medical Institute, Ashburn VA 20147, United States.

4: Present address: MRC Human Genetics Unit, Institute of Genetics and Cancer, University of Edinburgh, Western General Hospital, Crewe Road South, Edinburgh, EH4 2XU, United Kingdom.

5: Department of Genetics, University of Cambridge, Downing Street, Cambridge CB2 3EH, United Kingdom.

6: Present address: Josep Carreras Leukemia Research Institute, Department of Biomedicine, School of Medicine, University of Barcelona, Barcelona Spain.

7: Julius-Maximilians-Universität Würzburg, Faculty of Biology, Center for Computational and Theoretical Biology, Klara-Oppenheimer-Weg 32, Campus Hubland Nord, 97074, Würzburg, Germany.

8: Present address: Systems Bioengineering, MELIS, Universidad Pompeu Fabra, Barcelona, Spain.

* : corresponding author (silvia.munoz@ulpgc.es)

Key words: Wnt/β-catenin signalling, cell fate decision, mouse blastocyst, quantitative image analyses

ABSTRACT

Cell fate choice is a key event happening during preimplantation mouse development. From embryonic day 3.5 (E3.5) to E4.5, the inner cell mass (ICM) differentiates into epiblast (Epi, NANOG expressing cells) and primitive endoderm (PrE, GATA6, SOX17 and/or GATA4 expressing cells). The mechanism by which ICM cells differentiate into Epi cells and PrE cells remains partially unknown. FGF/ERK has been proposed as the main signalling pathway for this event, but it does not explain co-expression of NANOG and GAT6 or how the cell fate choice is initiated.

In this study, we investigate whether Wnt/β-catenin signalling also plays a role. To this end, we use two *in vitro* models based on inducible GATA6 expression: one in 2D, and another in 3D, namely ICM organoids. By combining these *in vitro* models with *in vivo* mouse embryos, chemical and classical genetics, and quantitative 3D immunofluorescence analyses, we propose a dual role for Wnt/β-catenin signalling.

We find that β-catenin, acting alongside FGF/ERK signalling, helps to guide the cell fate choice towards PrE. Additionally, by regulating GATA6 and GATA4 stability, β-catenin further facilitates this choice. To summarise, we observe that pathway activation promotes PrE differentiation, while its inhibition stalls it.

SUMMARY STATEMENT:

Wnt/β-catenin signalling promotes PrE fate in mouse preimplantation embryos.

INTRODUCTION

Early mammalian embryo preimplantation development involves two sequential cell fate decisions that provide the embryo with the essential machinery to implant and, subsequently, successful development until birth (reviewed in (White and Plachta, 2019)). During the first decision, a subset of cells differentiate into trophectoderm (TE) that will later form the embryonic portion of the placenta. The other cells (so-called inner cells mass, ICM, cells) will differentiate into epiblast (Epi, will become the embryo proper) or primitive endoderm (PrE, will form the yolk sac). Multiple studies have addressed how ICM cells differentiate into Epi or PrE cells. In mice, during the differentiation process, NANOG and GATA6 are co-expressed in ICM cells (Chambers et al., 2003; Chazaud et al., 2006; Messerschmidt and Kemler, 2010; Plusa et al., 2008; Saiz et al., 2016; Saiz et al., 2020; Schrode et al., 2015; Xenopoulos et al., 2015). Their mutual inhibition results in Epi or PrE fate differentiation: Epi cells maintain NANOG expression (downregulating GATA6 expression), while PrE cells keep GATA6 expression (downregulating NANOG expression) (Chazaud et al., 2006; Frankenberg et al., 2011). At later stages, PrE cells express other fate markers like GATA4, SOX17 and SOX7, and sort facing the embryo cavity (Artus et al., 2011). Our recent research has utilised single-cell quantitative immunofluorescence analysis (QIF) alongside three-dimensional neighbourhood analyses and mathematical modelling. This approach has underscored the importance of investigating cell fate decisions within the context of the entire ICM (Fischer et al., 2020; Fischer et al., 2023). Furthermore, we demonstrated that maternal factors such as age, obesity, and hyperglycaemia are associated with delays in these cell fate decisions(Lilao-Garzón et al., 2023).

The FGF/MAPK signalling pathway is the primary mechanism driving cell fate decision, as it promotes PrE fate while inhibiting Epi fate (Frankenberg et al., 2011; Guo et al., 2010; Kang et al., 2013; Kang et al., 2017; Messerschmidt and Kemler, 2010; Molotkov et al., 2017; Nowotschin et al., 2019; Ohnishi et al., 2013; Simon et al., 2020) (reviewed in (Soszyńska et al., 2019)). However, other signalling pathways also play significant roles. Specifically, active p38-Mapk14/11 is required for PrE differentiation (Thamodaran and Bruce, 2016). Additionally, PI3K/AKT signalling is active during preimplantation development, regulates NANOG and enables cells to respond to FGF (Geiselmann et al., 2024). We have previously hypothesised a potential role for Wnt/β-catenin signalling in this process (Muñoz-Descalzo et al., 2015)based on its function during the pluripotency and differentiation of the *in vitro* ICM counterpart—mouse embryonic stem cells (mESCs) (Faunes et al., 2013; Muñoz-Descalzo et al., 2013; Muñoz-Descalzo et al., 2015). In mESCs, β-catenin stabilises the pluripotent state by forming a complex with NANOG and OCT4 localised at the cell membrane; during differentiation, the complex is disassembled, and β-catenin is free to enter the nucleus to promote the transcription

of differentiation-related genes (Faunes et al., 2013; Muñoz-Descalzo et al., 2013; Zhang et al., 2013). (Anderson et al., 2017)

Previous studies have examined the potential role of Wnt/β-catenin *in vivo* during mouse preimplantation development. Maternally deposited β-catenin in the mouse oocyte is sufficient to successfully complete preimplantation development (Haegel et al., 1995). Consequently, materno-zygotic *β-catenin* mutant embryos were generated to study its function (de Vries, 2004). Initial studies suggested that the traditional mutant allele produced a truncated version of β-catenin (Brault et al., 2001; de Vries, 2004; Messerschmidt et al., 2016). For this reason, a new null allele was generated, and materno-zygotic *β-catenin* mutant embryos were analysed (Messerschmidt et al., 2016). These embryos showed defects in blastomere adhesion and size but did not display qualitative defects in lineage allocation. Likewise, other studies addressing a potential role for Wnt/β-catenin signalling during mouse preimplantation development using qualitative methods found no evidence of involvement in either blastocyst formation or cell fate allocation (Biechele et al., 2013; Xie et al., 2008).

Here, we explore the role of Wnt/β-catenin signalling during Epi vs PrE differentiation using quantitative methods. We use a combination of *in vitro* (2D and 3D) and *in vivo* models, alongside chemical and genetic modulation, coupled with data analyses based on quantitative immunofluorescence (QIF). Our detailed single cell quantitative analyses in multiple models allows us to propose that Wnt/β-catenin signalling promotes PrE fate, playing a role during cell fate allocation in mouse preimplantation embryos.

RESULTS

Membrane β-catenin is higher in Epi precursors compared to PrE precursors

During mouse embryonic stem cells (mESCs) differentiation membrane localised β-catenin is released and transcriptional activity is detected (Faunes et al., 2013). Given the embryonic origin of mESCs, we investigated the subcellular localisation of β-catenin in mouse preimplantation embryos, focusing on its relationship with the epiblast (Epi) and primitive endoderm (PrE) fate markers NANOG and GATA6, respectively (Figs. 1-2). In early (E3.5, 32-64 cells) and mid (E4.0, 65-90 cells) blastocysts, we observe high membrane β-catenin levels in ICM cells (cells co-expressing both NANOG and GATA6, N+G6+, Fig. 1A-B). In late blastocysts (E4.5, >90 cells), β-catenin levels remain high in the Epi cell (N+G6-) membranes and is downregulated in PrE (N-G6+) cell membranes (Fig. 1C). No obvious nuclear β-catenin can be observed, not even using a specific antibody against the transcriptionally active form of β-catenin (Fig. S1).

To examine possible differences depending on the developmental stage and cell fate decision progression, we measured membrane β-catenin levels between ICM (N+G6+), Epi (N+G6-) and PrE (N-G6+) cells in early, mid and late embryos (Fig. 2). In early embryos, all N+G6+ cells exhibit high membrane β-catenin levels (Fig. 2A-C). In mid blastocysts, membrane β-catenin levels are higher among N+G6- than between N+G6- cells and N-G6+ or N-G6+ cells (Fig. 2D-F). By late embryos, the differences observed in mid-blastocysts become more pronounced (Fig. 2G-I).

Altogether, these results align with our previously published β-catenin subcellular location in mESCs (Faunes et al., 2013): undifferentiated cells (ICM cells) have high levels of membrane β-catenin with no clear nuclear localization, while for differentiated cells, Epi cells retain high membrane β-catenin levels, whereas PrE cells show a decrease in membrane β-catenin.

Chemical modulation of Wnt/β-catenin signalling influences PrE/Epi fate *in vitro*

Our previous results in mESCs show that Wnt/β-catenin signalling is activated during differentiation (Faunes et al., 2013; Muñoz-Descalzo et al., 2013). Additional studies in mouse embryos and mESCs also indicated that activation of the pathway promoted PrE fate (Anderson et al., 2017; Nichols et al., 2009; Schroter et al., 2015). Altogether, this led us to propose that it may play a role in PrE differentiation (Muñoz-Descalzo et al., 2015).

To test the involvement of Wnt/β-catenin signalling in PrE differentiation, we used *tet::Gata6*-mCherry mESCs (Schroter et al., 2015). Briefly, to induce differentiation, NANOG expressing *tet::Gata6*-mCherry mESCs are treated with doxycycline (dox) for 6 hours to induce the expression of *Gata6*-mCherry allowing the cells to acquire an ICM-like state co-expressing NANOG and GATA6 (Fig. 3A). Following this induction, cells are cultured in mESCs medium without dox for 24 hours to allow their differentiation into Epi-like or PrE-like cells. To test the involvement of Wnt/β-catenin signalling in PrE- versus Epi-like fate differentiation, we cultured these cells throughout the experiment in the presence of Chi (a well-known Wnt/β-catenin signalling activator), or XAV (an inhibitor) (Fig. 3 and S2A (Huang et al., 2009; Ying et al., 2008)). To confirm induction of the PrE programme, we monitor SOX17 (S17) and GATA4 (G4) expression with quantitative immunofluorescence (QIF) analysis followed by population analysis (Fischer et al., 2020; Lou et al., 2014). We observe a clear effect in PrE differentiation after modulating Wnt/β-catenin signalling. Pathway activation increases the percentage of PrE-like cells (N-S17+ or N-G4+), which also exhibited higher expression levels of the PrE markers SOX17 and GATA4 (Fig 3B-C and S2B). Conversely, pathway inhibition produced opposite effects: a reduced percentage of PrE-like cells and lower S17 expression levels. The effects on the other cell-types are less pronounced: ICM-like (N+S17+ and N+G4+) and Epi-like (N+S17- and N+G4-) cells are influenced by signalling activation, but not by inhibition. The percentage of N-S17- and N-G4- cells

increase under both conditions. These cells might be in an advanced Epi-like fate where NANOG has been already downregulated, as previously suggested (Saiz et al., 2020). However, since these cells did not express any of the assessed markers, their fate remains ambiguous.

These results suggest that activation of Wnt/β-catenin signalling enhances PrE differentiation efficiency, whereas its inhibition hinders this process.

Wnt/β-catenin chemical modulation influences PrE/Epi fate *in vivo*

To examine whether modulation of Wnt/β-catenin signalling impacts PrE differentiation in vivo, we cultured early mouse preimplantation embryos (E3.5) in the presence of Wnt or XAV for 24h (Fig. 4 and S3) and monitored PrE differentiation using GATA4 as a marker. Consistent with *in vitro* observations, activation of Wnt/β-catenin signalling results in a higher proportion of PrE cells accompanied by increased GATA4 levels, at the expense of Epi cells (Fig. 4A-B and S3, upper panels). Conversely, inhibition of signalling with XAV reduced PrE differentiation, leading to an increase in Epi cells with higher NANOG levels (Fig. 4C-D and S3, lower panels). ICM cell proportion is also increased.

These results demonstrate that, *in vivo*, PrE and Epi fate decisions are also regulated by Wnt/β-catenin signalling. Activation of the pathway promotes PrE differentiation while hindering Epi fate. Conversely, inhibition decreases PrE differentiation and favours Epi fate.

Wnt/β-catenin signalling genetic inhibition influences PrE/Epi fate *in vitro*

To further investigate the effect of Wnt/β-catenin signalling on PrE differentiation, we generated new *β-catenin* mutant lines in the *tet::Gata6*-mCherry mESCs background (Schroter et al., 2015) (Fig. 5, Fig. S4-5). We used commercially available CRISPR gRNAs plasmids (see M&M). Several clones were generated and two (C5 and F1) were selected for further analyses (Fig. S4A-E). C5 was sent for sequencing, and it has a deletion spanning exons 4-5 (Fig. S4F), resulting in no detectable functional protein (Fig. S4G-H). As with the chemical inhibition of the pathway, we observe a decreased efficiency in PrE-like differentiation, but only when using GATA4 as a marker. Specifically, there is a lower proportion of PrE-like cells (N-G4+, Fig. 5B) and decreased expression levels of both GATA6 and GATA4 (Fig. S5). In the absence of β-catenin, we also detect a reduction in the proportion of Epi-like cells (N-G4+) and NANOG expression levels, likely due to its effect on NANOG stability or indicating an advanced Epi state (Muñoz-Descalzo et al., 2013; Saiz et al., 2020). There is also an increase in N-G6- (or N-G4-) cells that, as previously suggested, may reflect more advanced Epi-like cells.

We next used the newly generated *β-catenin* mutant line to generate ICM organoids, a three-dimensional *in vitro* system that mimics ICM differentiation into Epi and PrE (Mathew et al., 2019) (Fig. 6 and S6-7). *β-catenin* mutant ICM organoids exhibit no statistically significant differences in PrE/Epi-

like differentiation (Fig. 6A-C, regimes I, control, and II, mutant). However, we observe a defect in NANOG expressing cells upon analysing the 3D distribution of Epi- and PrE-like cells. Unlike wild-type ICM organoids, where high NANOG-expressing cells are found closer to the organoid centroid (Fig. 6D, black line (Mathew et al., 2019)), some high NANOG-expressing cells are in the periphery (Fig. 6D, red line). The absence of *β-catenin* does not affect the total cell number in the ICM organoids (Fig. S7A). Here we do not observe differences in NANOG or GATA6 expression levels (Fig. S7B) nor in GATA6 expressing cells distribution (Fig. S7C).

We next challenged the differentiation by generating ICM organoids chimeras by mixing *β-catenin* wild-type and mutant cells. To achieve this, we induce GATA6 expression in both cell lines prior to mixing (Fig. 6A, regime III). Under this conditions, *β-catenin* mutant cells preferentially differentiate into Epi-like fate. In contrast, wild-type cells predominantly differentiate into PrE-like fate (Fig. 6C). Notably, this approach rescued the defect observed in the distribution of NANOG-expressing cells. In chimeric organoids, high NANOG-expressing cells were no longer found at the periphery but were instead correctly localised near the organoid centroid (Fig. 6D, lower panel). Furthermore, NANOG and GATA6 expression levels decrease when comparing all the cells within the chimeric and wild-type ICM organoids. Similar reductions were observed when directly comparing wild-type and mutant cells within the chimeric ICM organoid (Fig. S7B).

Chimera experiments also allow determining whether β-catenin acts cell-autonomously or non-cell-autonomously. To test this, we induced GATA6 expression in wild-type cells before mixing them with uninduced *β-catenin* mutant cells, and vice versa (Fig. S6, regime IV and V, respectively). In both scenarios, we observe that PrE-like fate arises exclusively from induced GATA6 expressing cells, with Epi-like cells originating from the uninduced cells. When only *β-catenin* mutant cells were induced (regime V), we also observe a decrease in the percentage of PrE-like cells from *β-catenin* mutant cells. As a control, we generated 3D aggregates using uninduced wild-type and mutant *β-catenin* cells; in this case, we observe no PrE-like cells (Fig. S6, regime VI). Altogether, these findings indicate that PrE-like fate is acquired in a cell-autonomous manner from the induced cells. In other words, induced cells do not promote PrE fate to neighbouring uninduced cells.

In summary, genetic β-catenin inhibition in both 2D or 3D (ICM organoids) *in vitro* models of PrE differentiation leads to a reduced efficiency in PrE-like differentiation, favouring Epi-like fate. The effects are more pronounced in the 2D cell cultures compared to the ICM organoids. This disparity is likely attributable to mechanical factors or differences in the developmental stages represented by the two systems.

Wnt/β-catenin signalling genetic inhibition influences PrE/Epi fate *in vivo*

Maternally deposited β-catenin in the mouse oocyte is sufficient to successfully complete preimplantation development (de Vries, 2004; Messerschmidt et al., 2016). Hence, to investigate the role of β-catenin during this stage, we generated materno-zygotic (MZ) mutant embryos using the *ZP3*-Cre system (de Vries, 2004; Le Bin et al., 2014) with *β-catenin*$^{loxP/-}$ mice harbouring the *Ctnnb1*^{Tm2Kem} allele (deletion of exons 2-6) (Brault et al., 2001). The control littermates of the MZ embryos are heterozygous (Het) for *β-catenin* (see M&M). A previous report indicates that this allele produces a truncated protein version (Messerschmidt et al., 2016). However, our immunofluorescence analyses of MZ generated embryos with a polyclonal and a monoclonal antibody show no detectable signal (Fig. 7 and 8).

To assess the role of β-catenin during Epi vs PrE differentiation, MZ *β-catenin* mutant and Het embryos were stained for NANOG and GATA6, together with an antibody against β-catenin for genotyping (Fig. 7 and S8). In early MZ *β-catenin* mutant embryos, there is an increase in PrE differentiation (N-G6+), at the expense of ICM cells (N+G6+). This is likely due to reduced NANOG expression in N+G6+ cells (Fig. S8). However, in mid and late MZ *β-catenin* mutant embryos, a clear defect in PrE differentiation is observed, along with a higher proportion of cells remaining in an undifferentiated ICM cell state (N+G6+). In the mid MZ *β-catenin* mutant embryos, NANOG levels are reduced in Epi cells (N+G6-), and GATA6 levels are also reduced in ICM and PrE cells. In late MZ *β-catenin* mutant embryos, GATA6 levels are elevated in the still undifferentiated ICM cells.

In summary, in the absence of *β-catenin*, we observe defects in PrE differentiation: cell fate acquisition seems more efficient in early embryos, but then it stalls in mid and late embryos with a higher proportion of cells remaining undifferentiated.

Wnt/β-catenin and FGF/MAPK signalling cooperate to induce PrE fate

The main signalling pathway involved in this cell fate acquisition in mouse preimplantation embryos is FGF/MAPK signalling (Frankenberg et al., 2011; Guo et al., 2010; Kang et al., 2013; Kang et al., 2017; Messerschmidt and Kemler, 2010; Molotkov et al., 2017; Nowotschin et al., 2019; Ohnishi et al., 2013). Hence, we next investigated the relationship between FGF/MAPK and Wnt/β-catenin signalling in this process. To determine whether the defects in PrE differentiation in MZ β-catenin mutant late embryos could be rescued, we treated E3.5 embryos with FGF for 24 hours (Figs. 8A-B and S9A). Remarkably, activating FGF signalling in the absence of β-catenin effectively rescued the PrE differentiation defects. To gain deeper insight, we conducted the reversed experiment: we treated wild-type embryos with FGFRi to inhibit PrE differentiation and tested whether the activating Wnt/β-catenin signalling using Wnt3a could rescue these defects (Fig. S9B-C). Under these conditions, activation of Wnt/β-catenin signalling does not rescue the PrE differentiation defects.

dusp4 is a direct target of FGF/MAPK signalling (Gattiglio et al., 2023; Kalkan et al., 2019; Niwa et al., 2007) and acts as a negative-feedback regulator by dephosphorylating ERK (reviewed in (Caunt and Keyse, 2013)). During mouse preimplantation development, DUSP4 is accumulated following ERK phosphorylation in presumptive PrE cells (Azami et al., 2019). To further investigate the interplay between FGF/MAPK and Wnt/β-catenin signalling, we examined whether the absence of β-catenin influences DUSP4 expression (Fig. 8C-D and Fig. S9D). Surprisingly, we observe an increased number of N-DUSP4+ cells in early MZ *β-catenin* mutant embryos (at the expense of N+DUSP4+). In mid embryos, there is an increase of N+DUSP4+ cells (at the expense of N-DUSP4- cells) which clearly show altered DUSP4 expression levels.

Altogether, these results suggest FGF/MAPK signalling acts downstream or in parallel with Wnt/β-catenin signalling during PrE differentiation. Furthermore, in the absence of *β-catenin*, DUSP4 accumulates and likely inhibits FGF/MAPK signalling activation.

β-catenin acts independently of Wnt/β-catenin signalling activation during PrE differentiation

Previous studies using scRNAseq data suggested that Wnt/β-catenin signalling is active in Epi cells of E4.5 embryos (Athanasouli et al., 2023). However, the analysis did not cover the differentiation process from E.25 to E4.5 embryos. To investigate Wnt/β-catenin signalling activity throughout ICM differentiation towards PrE and Epi fates, we re-analysed previously published scRNAseq data (Fig. 9A) (Linneberg-Agerholm et al., 2024; Nowotschin et al., 2019). In ICM cells (E3.25 and E3.5 embryos), there is high expression of the Wnt/β-catenin signalling negative regulators *gsk3a* and *apoe*, as well as the positive regulator *fn1*. This pattern persists in E3.5 Epi cells, which becomes even more pronounced in E4.5 Epi cells. In these cells, another Wnt positive regulator, *lef1*, is also highly expressed. In PrE cells, both *gsk3a* and *apoe* are expressed (in E3.5 and E4.5 embryos); the key differences between ICM and Epi cells lie in the high expression of *dkk1*, and the lower expression of *fn1*. As previously suggested (Athanasouli et al., 2023), these results point towards Wnt/β-catenin signalling being activated in Epi cells but inhibited in PrE cells.

We also analysed whether *β-catenin* (*ctnnb1*) expression is differentially regulated during early development (Fig. S10A). As previously reported, we observe that *β-catenin* is expressed at similar levels across all stages and fates, validating the need of materno-zygotic mutant embryos to investigate its role (de Vries, 2004; Messerschmidt et al., 2016). Interestingly, the only statistically significant difference in expression levels occurs between ICM and PrE cells in E3.5 embryos, suggesting a role for β-catenin in PrE cells. For comparison, the expression levels of other fate-specific genes are also shown (Fig. S10B). During this analysis, we identified two genes which exhibit clear upregulation in PrE cells, namely *sparc* and *aqp8*. While these genes have been previously studied in

the context of mouse preimplantation development, no research has been conducted to investigate points towards a role in PrE vs Epi differentiation (Barcroft et al., 2003; Latham and Howe, 1991; Richard et al., 2003).

The scRNAseq data analyses are at odds with the results shown in this study, which suggest that β-catenin activates PrE fate. Our previous work showed a role for β-catenin in the maintenance of pluripotency by regulating pluripotency markers via protein complexes stabilities, rather than promoting their transcriptional activation via Wnt/β-catenin signalling activation (Faunes et al., 2013; Muñoz-Descalzo et al., 2013). Within this context, we hypothesised that β-catenin might exert a similar function. To test this hypothesis, we measured the stability of NANOG, GATA6 and GATA4 using quantitative immunofluorescence analysis after promoting Epi- or PrE-like fate in the 2D *β-catenin* wild-type or mutant cells while blocking translations (adding cycloheximide) for 0, 2, 4 or 6h to the *tet::Gata6*-mCherry mESCs (Fig. 9B-E and S11). To estimate NANOG, GATA6 and GATA4 stability, we fitted a first-order decay model using the measured expression levels (dashed lines in Fig. 9C-E). Upon levels normalization under both genetic backgrounds, we observed no changes in NANOG stability (Fig. 9C). However, both GATA6 and GATA4 stabilities are significantly affected by the absence of β-catenin (Fig. 9D-E).

This suggests that β-catenin contributes to PrE differentiation post-transcriptionally by stabilising GATA6 and GATA4.

DISCUSSION

Previous studies did not identify a role for Wnt/β-catenin signalling during mouse preimplantation development and Epi versus PrE differentiation (Biechele et al., 2013; Brault et al., 2001; de Vries, 2004; Haegel et al., 1995; Messerschmidt et al., 2016; Xie et al., 2008). This was likely due to the use of qualitative rather than quantitative approaches. We have previously proposed a role in the process based on mESCs studies and given the embryonic origin of these (Faunes et al., 2013; Muñoz-Descalzo et al., 2013; Muñoz-Descalzo et al., 2015). Furthermore, other studies have hinted at a potential role: in the *in vitro* PrE-like differentiation model, the addition of Chi to the culture enhances PrE-like differentiation and increases the number of PrE cells in the embryo (Nichols et al., 2009; Schroter et al., 2015). Furthermore, Wnt, in combination with ActA, induces PrE in naïve pluripotent cells (Anderson et al., 2017). Here, we quantitatively analyse the influence of Wnt/β-catenin signalling during mouse Epi and PrE differentiation using 2D and 3D *in vitro* models, as well as *in vivo* models. To this end, we apply chemical and genetic activation or inhibition of the pathway. In summary, we find that activation of the pathway enhances PrE differentiation, whereas its inhibition stalls it. For this activity Wnt/β-catenin cooperates with FGF/MAPK signalling.

In this study we use three biological systems (2D cell culture and ICM organoids), and embryos to manipulate Wnt/β-catenin signalling and investigate its role during cell fate allocation. Our results allow us to propose that it promotes PrE differentiation. The different systems allow us to address various aspects of the process, as recently shown with FGF/MAPK response in mESCs and embryos (Perera and Brickman, 2024). The 2D system is based on mESCs genetically "forced" to differentiate into PrE-like cells via GATA6 overexpression. Consequently, the results we observe represent a mixture of the effects that Wnt/β-catenin signalling has on pluripotency and differentiation (Faunes et al., 2013; Muñoz-Descalzo et al., 2013; Wray et al., 2011). Increasing β-catenin levels (via the addition of Chi) inhibits pluripotency exit, resulting in the observation of more ICM-like cells (due to ectopic GATA6 expression). In cells primed for differentiation, higher β-catenin promotes pluripotency exit and, under this condition, we observe more PrE-like cells. For the opposite situation, we have two scenarios: one with lower β-catenin levels (XAV treatment) and the other with no β-catenin at all (mutant cells). In both cases we observe a reduction in PrE-like differentiation efficiency and an increase in cells expressing neither Epi (NANOG), nor PrE markers (SOX17, GATA4). These later cells might reflect cells differentiating into more advanced embryonic fates (Saiz et al., 2020). The key difference between these two scenarios lies in the NANOG expressing cells (Epi-like cells): under XAV treatment, there is sufficient β-catenin to support the presence of these cells; however, in the absence of β-catenin, we find fewer Epi-like cells, as NANOG decreases its stability in mESCs or maybe reflecting a more advanced Epi state (Muñoz-Descalzo et al., 2013; Saiz et al., 2020).

In the ICM organoids, we force cells to differentiate while forming a 3D structure resembling the ICM (Mathew et al., 2019). In this system, we only observe a defect in PrE-like differentiation when mixing *β-catenin* wild-type and mutant cells to generate a chimeric ICM organoid. In the absence of β-catenin, cells preferentially differentiate into Epi-like cells, with wild-type cells comprising most PrE-like cells. ICM organoids composed entirely of mutant cells do not exhibit any differentiation defect, but show altered cell distribution, with Epi-like cells reaching the periphery of the organoid. This may reflect defects in cell adhesion within mutant PrE-like cells. Interestingly, this is the only adhesion-related defect identified in our study, despite the role of β-catenin at the adherens junctions (Messerschmidt et al., 2016; Moghe et al., 2025; Muñoz-Descalzo et al., 2015; Yanagida et al., 2022).

Finally, the results obtained from the *in vivo* system (i. e., the embryo) allow us to hypothesise how Wnt/β-catenin signalling is involved in mouse preimplantation cell fate decisions at different stages. We observe a clear defect in materno-zygotic *β-catenin* mutant embryos in PrE differentiation, alongside an increase in undifferentiated ICM cells co-expressing NANOG and GATA6 (in mid and late embryos), which has only partially been observed in the *in vitro* models. This leads us to propose that, in the absence of β-catenin, the cell fate acquisition is delayed. In the *in vitro* systems, cells do have

time to process new differentiation directions and transit through different states (naïve, formative, primed). However, the mouse embryo has a finite time to progress through development till birth. Thus, it is unsurprising that the effects of Wnt/β-catenin vary, given its role in cell state transitions in mouse (Kalkan et al., 2017; Kalkan et al., 2019; Smith, 2017).

The mechanism by which Wnt/β-catenin signalling contributes to the transition from ICM to PrE/Epi fate is likely complex and context dependent as suggested for FGF/MAPK signalling (Perera and Brickman, 2024). In our study, we observe at least two ways by which Wnt/β-catenin signalling is involved. The first one involves the crosstalk with FGF/MAPK signalling. Our results indicate that Wnt/β-catenin signalling acts downstream of or in parallel with FGF. Interestingly, mouse preimplantation development is not the only system where these two pathways interact. Both in basal cells of the trachea and in neuromesodermal progenitors these two pathways are active (Hou et al., 2019; Turner et al., 2014). The second mechanism is via GATA6 and GATA4 protein stability. Given the autoactivation of *gata6* expression during PrE differentiation by binding to its own promoter but also to the *gata4* promoter (Meng et al., 2018; Wamaitha et al., 2015), the reduced GATA6 stability in the absence of β-catenin explains the observed defects (lower GATA6/4 levels and decreased PrE differentiation). Surprisingly, just 2h after stopping translation (CHX treatment), both GATA6 and GATA4 levels decrease significantly, indicating that their dynamics are notably fast in the absence of β-catenin. These two mechanisms are not independent, they likely coexist in the process.

Interesting findings emerge from the analysis of DUSP4. *dusp4* expression and protein levels oscillate during somitogenesis (Niwa et al., 2007) and act as a negative-feedback regulator of FGF/MAPK signalling by dephosphorylating ERK (reviewed in (Caunt and Keyse, 2013)). This regulation also occurs during PrE differentiation (Azami et al., 2019; Raina et al., 2022; Simon et al., 2020). Oscillations in FGF/MAPK signalling have been observed in mouse embryonic stem cells (Raina et al., 2022), in cells exiting pluripotency (Arekatla et al., 2023), and in mouse blastocysts (Simon et al., 2020). Specifically, studies on pluripotency exit demonstrate that, rather than MAPK dynamics, it is the cumulative ERK activity experienced by the cells that determines the outcome (Arekatla et al., 2023). Additionally, FGF promotes more cells entering an oscillatory regime, which would safeguard cells from spurious signal activation (Raina et al., 2022). While no *dusp4* oscillations have been reported during mouse preimplantation development, the presence of distinct high- and low-*dusp4*-expressing cell populations in PrE cells of E3.5 embryos suggests a similar behaviour in this system. In our study, we observe different DUSP4 levels as development progresses as published before (Azami et al., 2019), which are altered in β-catenin mutant embryos. It is tempting to propose that Wnt/β-catenin might regulate DUSP4 activity and, in turn, influence MAPK signalling oscillations. Indeed, in the early

MZ *β-catenin* mutant embryos, we observe an increase in DUSP4+ cells and more PrE cells; in the mid embryos, a new population of cells emerges in which both NANOG and DUSP4 are coexpressed.

Overall, we can propose the working model shown in Figure 10, which combines our results (blue lines) with previous finding (black lines). In wild-type ICM cells FGF/MAPK signalling oscillates (Fig. 10A (Arekatla et al., 2023; Pokrass et al., 2020; Raina et al., 2022; Simon et al., 2020)). High FGF/MAPK signalling (upper part in Fig. 10A) activates GATA6 and inhibits NANOG (via phosphorylation through ERK) (Kim et al., 2014; Meng et al., 2018); GATA6 reinforces PrE fate by promoting its own expression (Meng et al., 2018; Wamaitha et al., 2015), while inhibiting Epi fate by repressing *nanog* (Thompson et al., 2022; Wamaitha et al., 2015). FGF/MAPK signalling promotes *dusp4* expression (Azami et al., 2019; Gattiglio et al., 2023; Kalkan et al., 2019; Niwa et al., 2007), which acts as a negative-feedback regulator by dephosphorylating ERK during PrE differentiation (Azami et al., 2019; Raina et al., 2022; Simon et al., 2020). This negative feedback would result into low FGF/MAPK signalling (lower part in Fig. 10A); under these conditions, NANOG phosphorylation decreases, leading to an increase NANOG levels, inhibition of *gata6* expression (Singh et al., 2007), and progression towards Epi fate. In the absence of β-catenin (Fig. 10B), GATA6 stability decreases and DUSP4 is accumulated. This would result in reduced FGF/MAPK signalling activation, decreased ERK activity, further diminished GATA6 activity, increased NANOG activity and, consequently, reduced PrE fate.

FIGURE LEGENDS

Figure 1: β-catenin localises in cell membranes in mouse preimplantation embryos. Representative single confocal images of early, mid and late mouse blastocysts stained with antibodies against GATA6 (green), total β-catenin (red) and NANOG (magenta), DAPI (blue) was used to stain nuclei. Higher magnification images are above the whole embryo images. Scale bar: 50 μm.

Figure 2: Membrane β-catenin quantification during cell fate acquisition. (A, D and **G)** Representative single confocal images of early, mid and late mouse blastocysts stained with antibodies against total β-catenin (white), GATA6 (green), and NANOG (magenta), DAPI (blue) was used to stain nuclei. Scale bar: 50 μm. **(B, E** and **H)** Fluorescence intensity representation from the confocal images using ARIVIS software. The heat map represents the intensity of the indicated markers (blue for low, green for medium, red for high). **(C, F** and **I)** Profile plots showing the variation in fluorescence intensity across different lines drawn on confocal images using ImageJ. Grey lines show the profile between ICM (N+G6+) cells, magenta lines are between Epi cells (N+G6-) cells, green lines are between PrE cells (N-G6+) cells, and black lines are between Epi and PrE cells (N+G6-/N-G6+).

Figure 3: Chemical Wnt/b-catenin signalling modulation influences PrE fate *in vitro.* (A) Treatment regime of *tet::Gata6*-mCherry mESCs. **(B)** Representative single confocal images of control (first row),

Chi treated (central), or XAV treated (bottom) cells stained with antibodies against SOX17 (green), GATA4 (white) and NANOG (magenta), DAPI (blue) was used to stain nuclei. Scale bar: 50 μm. **(C)** Population analyses show the mean percentage of N-S17-, N+S17+, N+S17- and N-S17+ (left) or N-G4-, N+G4+, N+G4- and N-G4+ (right) cells. Z-test two-tailed hypothesis with Bonferroni correction, *: p<0.1; **p<0.05. The comparisons were made only against the control regime. n is the number of analysed cells.

Figure 4: Chemical Wnt/b-catenin signalling modulation influences PrE fate *in vivo.* (A, C) Representative single confocal images of control (first rows), and Wnt3a- or XAV-treated (bottom rows) early mouse embryos (E3.5) for 24h and stained with antibodies against active β-catenin (ABC, green), GATA4 (white) and NANOG (magenta), DAPI (blue) was used to stain nuclei. Scale bar: 50 μm. **(B, D)** Population analyses show the mean percentage of N-G4-, N+G4+, N+G4- and N-G4+ cells. Z-test two-tailed hypothesis, *: p<0.05. n is the number of analysed embryos.

Figure 5: Genetic Wnt/b-catenin signalling inhibition hinders PrE fate *in vitro* (2D). (A) Representative single confocal images of *β-catenin*$^{+/+}$ *tet::Gata6*-mCherry (above) and *β-catenin*$^{-/-}$ (below) *tet::Gata6*-mCherry mESCs after inducing PrE differentiation and stained with antibodies against GATA6 (green), GATA4 (white) and NANOG (magenta), DAPI (blue) was used to stain nuclei. Scale bar: 50 μm. **(B)** Population analyses show the mean percentage of N-G6-, N+G6+, N+G6- and N-G6+ (left) or N-G4-, N+G4+, N+G4- and N-G4+ (right) cells. Z-test two tailed-hypothesis, *: p<0.05.

Figure 6: Genetic Wnt/b-catenin signalling inhibition hinders PrE fate *in vitro* (3D). (A) ICM organoids formation regime using *β-catenin*$^{+/+}$ or *β-catenin*$^{-/-}$ *tet::Gata6*-mCherry mESCs after inducing PrE differentiation (I and II, respectively). Chimeric ICM organoids were formed by mixing equal cell numbers of induced (6h Dox-treated cells) *β-catenin*$^{+/+}$ and *β-catenin*$^{-/-}$ *tet::Gata6*-mCherry cells (III). **(B)** Representative single confocal images of the ICM organoids generated in each regime and stained with antibodies against total β-catenin (white), GATA6 (green), and NANOG (magenta) , DAPI (blue) was used to stain nuclei. Scale bar: 50 μm. **(C)** Population analysis of the different ICM organoids cell composition indicating the mean percentage of N-G6-, N+G6+, N+G6- and N-G6+ cells. Z-test two tailed-hypothesis between I and II or III (with Bonferroni correction), and between *β-catenin*$^{+/+}$ and *β-catenin*$^{-/-}$ cells in III, *: p<0.05. n indicates the number of analysed ICM organoids. **(D)** Mean level of NANOG (vertical axis) versus the distance to the ICM centroid (horizontal axis, binned in 5 μm groups) for *β-catenin*$^{+/+}$ (grey) or *β-catenin*$^{-/-}$ (red) cells in ICM organoids of I and II (above) or III (below) regime.

Figure 7: Genetic Wnt/b-catenin signalling inhibition hinders PrE fate *in vivo.* (A) Representative single confocal images of *β-catenin*$^{+/-}$ *or* materno-zygotic (MZ) *β-catenin*$^{-/-}$ mutant embryos of the indicated stages stained with antibodies against total β-catenin (white), GATA6 (green), and NANOG

(magenta), DAPI (blue) was used to stain nuclei. Shown embryos from the same developmental stage were immunostained, imaged and processed together. Scale bar: 50 μm. **(B)** Population analysis shows the mean percentage of N-G6-, N+G6+, N+G6- and N-G6+ cells. Z-test two-tailed hypothesis, *: p<0.1, **<0.05. n is the number of analysed embryos.

Figure 8: Wnt/β-catenin signalling cooperates with FGF/MAPK signalling in cell fate decisions in early mouse embryos. (A) Representative single confocal images of *β-catenin*$^{+/-}$ *or* materno-zygotic (MZ) *β-catenin*$^{-/-}$ mutant early embryos cultured in control or FGF4-containing medium for 24h and stained with antibodies against active β-catenin (ABC, green), GATA4 (white) and NANOG (magenta), DAPI (blue) was used to stain nuclei. Scale bar: 50 μm. **(B)** Population analysis indicating the mean percentage of N-G4-, N+G4+, N+G4- and N-G4+ cells. The statistical comparison was made against the control treatment. Z-test two-tailed analysis with Bonferroni correction, *: p<0.05. n is the number of analysed embryos. **(C)** Representative single confocal images of freshly flushed *β-catenin*$^{+/-}$ *or* materno-zygotic (MZ) *β-catenin*$^{-/-}$ mutant early embryos and stained with antibodies against active β-catenin (white), DUSP4 (green), NANOG (magenta), and DAPI (blue) was used to stain nuclei. Scale bar: 50 μm. **(D)** Population analysis indicating the mean percentage of N-DUSP4-, N+DUSP4+, N+ DUSP4 - and DUSP4 + cells. The statistical comparison was made against the control treatment. Z-test two-tailed analysis, *: p<0.05. n is the number of analysed embryos.

Figure 9: β-catenin acts independently of Wnt/β-catenin signalling activation during PrE differentiation via GATA6 and GATA4 turnover regulation. (A) scRNAseq expression analyses of Wnt/β-catenin signalling positive (*fn1, lef1, tcf7* and *lgr4*) and negative regulators (*gsk3a, apoe, dkk1* and *znrf3*) in ICM cells from E3.25 embryos (left), and Epi and PrE lineages in E3.5 and 4.5 embryos (right). **(B)** Treatment regime of wild-type and mutant *β-catenin* mutant *tet::Gata6*-mCherry mESCs to measure NANOG, GATA6 and GATA4 half-lives. **(C-E)** Average levels and standard error of NANOG (C), GATA6 (D), and GATA4 (E) normalised to levels at 0h. Wild-type cells levels are in black, and mutant cells levels are in red. Dashed lines correspond to the best fit exponential decay model using the experimental data from wild-type and mutant cells, respectively. Shading shows the 90% confidence bands.

Figure 10: Working model for the role of Wnt/β-catenin during early mouse preimplantation embryo cell fate decision. Top scheme represents the wild-type situation with previously described relationships in black. The effects of the pathway on the process identified in this study are in blue. The bottom scheme represents how cell fate decision is affected in the absence of *β-catenin* (red lines), increasing or decreasing line weights or letter size accordingly. For simplicity transcriptional and posttranslational effects are not depicted differently. See main text for details.

SUPPLEMENTARY FIGURE LEGENDS

Figure S1: Active β-catenin localises in cell membranes in mouse preimplantation embryos. Representative single confocal images of early, and late mouse blastocysts stained with antibodies against GATA6 (green), active β-catenin (red), OCT4 (magenta), DAPI (blue) was used to stain nuclei. Scale bar: 50 μm.

Figure S2: Chemical Wnt/b-catenin signalling modulation influences PrE fate *in vitro.* (A) Representative single confocal images of *tet::Gata6*-mCherry cells cultured under the indicated regimes in Fig. 3A and stained with an antibody against total β-catenin to reveal the inhibitors' effect. Scale bar: 50 μm. **(B)** Scatter plots showing the quantitative single cell analyses of the indicated markers in the indicated cell types cultured in the different regimes shown in Fig. 3. Red line shows the mean expression level. Mann-Whitney test with Bonferroni correction, *: p<0.05,. The statistical comparison was made against the control regime. n indicates the number of analysed cells.

Figure S3: Chemical Wnt/b-catenin signalling activation promotes PrE fate *in vitro.* Scatter plots showing the quantitative single cell analyses of the indicated markers in the indicated cell types. Red line shows the mean expression level. Mann-Whitney test, *: p<0.05. n is the number of analysed cells.

Figure S4: *β-catenin*$^{-/-}$ *tet::Gata6*-mCherry mESCs characterisation. (A) NCBI scheme (*Mus musculus* strain C57BL/6J chromosome 9, GRCm39 gi|1877089960|ref|NC_000075.7|) of *ctnnb1* gene showing the position of gRNA´s used to generate the mutant cell line (red). Primers´ position used to screen the generated clones (blue) are also indicated. **(B)** Schematic diagram of the β-catenin protein structure with functional domains. The gRNAs positions are indicated. **(C)** β-catenin protein sequence with gRNAs shown in red. **(D)** PCR results using the primers shown in (A) using control *β-catenin*$^{+/+}$ (C4 clone) and *β-catenin*$^{-/-}$ (C5, left, and F1, right, clones) cells´ genomic DNA. **(E)** Population analyses of control *β-catenin*$^{+/+}$ (C4 clone) and *β-catenin*$^{-/-}$ (F1 clone) cells indicating the mean percentage of N-G6-, N+G6+, N+G6- and N-G6+ (left) or N-G4-, N+G4+, N+G4- and N-G4+ (right) cells. Z-test two tailed-hypothesis, *: p<0.05. **(F)** *ctnnb1* nucleotide coding sequence with gRNAs shown in red. The different coding exons are shown in alternating colours (black and green). The blue box shows the deleted region in C5 clone. **(G)** Representative single confocal images of *β-catenin*$^{+/+}$ *tet::Gata6*-mCherry (above) and *β-catenin*$^{-/-}$ *tet::Gata6*-mCherry (C5 clone) mESCs with antibodies against NANOG (green), OCT4 (red) and total β-catenin (white), DAPI (blue) was used to stain nuclei. Scale bar: 50 μm. **(H)** Western blot analysis of *β-catenin*$^{+/+}$ and *β-catenin*$^{-/-}$ (C5 clone) mESCs total protein extracts using total β-catenin antibody. An antibody against GAPDH was used as loading control.

Figure S5: Genetic Wnt/b-catenin signalling inhibition hinders PrE fate *in vitro* (2D). Scatter plots showing the quantitative single cell analyses of the indicated markers in the indicated cell types shown

in Fig. 4. Red line shows the mean expression level. Mann-Whitney test, *: p<0.05. n is the number of analysed cells.

Figure S6: Genetic Wnt/b-catenin signalling inhibition hinders PrE fate *in vitro* (3D). (A) Complete ICM organoids formation regime using *β-catenin*$^{+/+}$ or *β-catenin*$^{-/-}$ of *tet::Gata6*-mCherry mESCs after inducing PrE differentiation (I and II, respectively). Chimeric ICM organoids were formed by mixing induced *β-catenin*$^{+/+}$ with uninduced *β-catenin*$^{-/-}$ *tet::Gata6*-mCherry cells (III), or induced *β-catenin*$^{-/-}$ with uninduced *β-catenin*$^{+/+}$ *tet::Gata6*-mCherry cells (IV). Chimeric aggregates with uninduced *β-catenin*$^{+/+}$ and *β-catenin*$^{-/-}$ of *tet::Gata6*-mCherry cells were also generated as control. **(B)** Representative single confocal images of the ICM organoids generated in each regime and stained with antibodies against total β-catenin (white), GATA6 (green) and NANOG (magenta), DAPI (blue) was used to stain nuclei. Scale bar: 50 μm. **(C)** Population analysis of the different ICM organoids (or aggregates) indicating the mean percentage of N-G6-, N+G6+, N+G6- and N-G6+ cells. Z-test two tailed-hypothesis between I and II, and between *β-catenin*$^{+/+}$ and *β-catenin*$^{-/-}$ cells in III, IV, V, and VI; *: p<0.05. n indicates the number of analysed ICM organoids.

Figure S7: Genetic Wnt/b-catenin signalling inhibition hinders PrE fate *in vitro* (3D). (A) Scatter plot showing the total cell number in each individual analysed ICM organoid. Red line shows the mean cell number. Mann-Whitney tests between I and II or III, and between *β-catenin*$^{+/+}$ and *β-catenin*$^{-/-}$ cells in III do not show a statistically significant difference at a significance level of p<0.05. **(B)** Scatter plots showing the quantitative single cell analyses of the fate markers in the indicated cell types shown in Fig. 5. Red line shows the mean expression level. Mann-Whitney test between I and II or III (with Bonferroni correction), and between WT and mutant cells within III, *: p<0.05. n is the number of analysed cells. **(C)** Mean level of GATA6 (vertical axis) versus the distance to the ICM centroid (horizontal axis, binned in 5 μm groups) for ICM organoid *β-catenin*$^{+/+}$ (grey) or *β-catenin*$^{-/-}$ (red) cells in ICM organoids of I and II (above) or III (below) regime.

Figure S8: Genetic Wnt/b-catenin signalling inhibition hinders PrE fate *in vivo.* Scatter plots showing the quantitative single cell analysis of the fate markers in the indicated cell types shown in Fig. 7B. Red line shows the mean expression level. Mann-Whitney test between marker levels of cells within the same stage, *: p<0.05. n is the number of analysed cells.

Figure S9: Wnt/β-catenin signalling cooperates with FGF/MAPK signalling in cell fate decisions in early mouse embryos. (A) Scatter plots showing the quantitative single cell analysis of the fate markers in the indicated populations in cells shown in Fig. 8B. Red line shows the mean expression level. Mann-Whitney test with Bonferroni correction, *: p<0.05. n is the number of analysed cells. **(B)** Population analysis indicating the mean percentage of N-G4-, N+G4+, N+G4- and N-G4+ cells in wild-

type embryos cultured in control, FGFRi, Wnt3a or FGFRi+Wnt3a-containing medium for 24h. Mann-Whitney test, *: p<0.05. n is the number of analysed cells. **(C)** Scatter plots showing the quantitative single cell analysis of the fate markers in the indicated populations in cells shown in B. Red line shows the mean expression level. Mann-Whitney test with Bonferroni correction, *: p<0.05. n is the number of analysed cells. **(D)** Scatter plots showing the quantitative single cell analysis of the indicated markers in the indicated populations in cells shown in Fig. 8D. Mann-Whitney test, *: p<0.05. n is the number of analysed cells.

Fig. S10: Single cell expression analyses of relevant genes during mouse preimplantation development. (A) *ctnnb1* expression levels at the indicated stages and cell types. Notice the statistically significant higher expression in PrE cells vs ICM cells in E3.5 embryos. **(B)** *dusp4*, *gata6*, *gata4* and *nanog* levels. Notice *dusp4* higher expression in PrE cells in E3.5 embryos, with clearly two populations present (one with high expression and another with low expression). The presence of a high and low expression population in these genes can only be found in *gata4* and *nanog* in the same cell type and stage. **(C)** *sparc* and *apq8* expression levels. These genes are the highest expressed genes in PrE cells, especially in E3.5 and 4.5 embryos. t-test independent samples with Bonferroni correction. * p <= 0.05. For simplicity, only relevant statistical comparisons are shown.

Fig. S11: β-catenin absence accelerates GATA6 and GATA4 turnover. (A) Population analysis of cells treated with CHX for the indicated time showing the mean percentage of N-G6-G4- (yellow), ICM-like cells (grey, N+G6+G4, N+G6+G4- or N+G6-G4+), Epi-like cells (magenta, N+G6-G4-) and PrE-like cells (green-blue, N-G6+G4-, N-G6-G4+ or N-G6+G4+). **(B)** Average levels and standard error of NANOG (magenta), GATA6 (green), and GATA4 (blue) normalised to levels at 0h. Wild-type cells levels are in darker colours, and mutant cells levels are in lighter colours. Lines correspond to the best fit exponential decay model using the experimental data from wild-type(continuous) and mutant cells (dashed).

MATERIALS AND METHODS

Mice and embryos

Mouse work was conducted following National and European regulations (RD 1201/2005, Law 32/2007, EU Directive 2010/63/EU), were approved by the Animal Ethics Committee of the ULPGC and were authorised by the competent authority of the Canary Islands Government (reference number: OEBA-ULPGC 08/2018). Initial mouse work in this project was approved by the University of Bath Animal Welfare and Ethical Review Body (AWERB) and undertaken under a UK Home Office license (PPL 30/3219) in accordance with the Animals (Scientific Procedures) Act incorporating EU Directive 2010/63/EU. Mice were maintained under a 14h light/10h dark cycle with food and water supplied *ad libitum*.

Mouse strains: CD1, and Swiss as wild-type strains. *Zp3*-Cre (C57BL/6-Tg(Zp3-cre)93Knw/J, JAX stock Nº: 003651) (De Vries et al., 2000); *Sox2*-Cre (B6.Cg-*Edil3*$^{Tg(Sox2\text{-}cre)1Amc}$/J, JAX stock Nº: 008454) (Hayashi et al., 2002); β-catenin$^{loxP/loxP}$ (B6.129-*Ctnnb1*^{tm2Kem}/KnwJ, JAX stock Nº: 004152) (Brault et al., 2001); β-catenin$^{+/-}$ (generated in house by mating β-catenin$^{loxP/loxP}$ with *Sox2*-Cre). Generation of materno-zygotic β-catenin mutant embryos was done as in (Le Bin et al., 2014).

Mouse genotyping primers were: β-catFLOXRM41 (AAGGTAGAGTGATGAAAGTTGTT), β-catFLOXRM42 (CACCATGTCCTCTGTCTATTC), β-cat$^{+/-}$ RM68 (AATCACAGGGACTTCCATACCAG),β-cat$^{+/-}$ RM69 (GCCCAGCCTTAGCCCAACT), Cre-oIMR 1084 (GCGGTCTGGCAGTAAAAACTATC), Cre-oIMR 1085 (GTGAAACAGCATTGCTGTCACTT), Cre-oIMR 7338 (CTAGGCCACAGAATTGAAAGATCT) and Cre-oIMR 7339 (GTAGGTGGAAATTCTAGCATCATCC).

Embryos used for this study were obtained via natural mating and flushed using M2 medium (Embryomax®; Millipore, Ref. MR-015-D). For culture, embryos were flushed at E3.5 and cultured in KSOM (Millipore, Ref. MR-121-D) at 37°C and 5% CO_2. Small molecules used were: Chiron9901 (Eurodiagnostico HY-10182, 3 µM), Wnt-3a (R&D, 1324-WN-002, 200ng/ml), XAV939 (R&D, 3740, 1µM), FGF2 (R&D, 233-FB-025, 500ng), FGFRi (AZD4547, Abcam, 1 µM) and PD035901 (TOCRIS, 4192, 1µM) were added one hour before starting the *ex vivo* culture to equilibrate the medium in the incubator.

Mouse embryonic stem cell (mESC) lines

*tet::*GATA6mCherry mESCs were kindly provided by Christian Schröter (Schroter et al., 2015). A truncated β-catenin GATA6 inducible cell line was obtained by CRISPR mutation using ready-made plasmids from Santa Cruz (sc-419477) formed by three different gRNA (one: ATGAGCAGCGTCAAACTGCG; two: AGCTACTTGCTCTTGCGTGA; three: AAAATGGCAGTGCGCCTAGC). *tet::*Gata6-mCherry mESCs were transfected chemically using the transfection reagent (Santa Cruz, sc-

395739) and transfection medium (Santa Cruz, sc-108062). Transfected mESCs were sorted based on GFP expression using a FACS Aria (BD Biosciences) 8 hours after transfection. The GFP fluorescence threshold was achieved using non-transfected cells as control. GFP positive cells were grown on iMEFs coated plates. Individually picked clones were screened using genomic PCR with primers designed for the 3 gRNA included in the transfected plasmid (F: CTGGCAGCAGCAGTCTTACT, R: GCACCGTACTGTACACACAGA). Sequencing data indicated that the F1 *β-catenin* mutant clone was not pure and was mixed with wild-type cells. Hence, unless otherwise indicated in the figures, only results from the C5 clone are shown in comparison with a C4 untransfected clone (wild-type control cells). mESCs culture was performed as previously described (Muñoz-Descalzo et al., 2013).

ICM organoids

ICM organoids were generated using as previously published, using 50 cells as starting population in ultra-low 96-well round bottom plates (Mathew et al., 2019). To generate the chimeric ICM organoids, 25 cells or each used cell genotype and or treatment was used to obtain a total of 50 cells used as starting number.

mESCs, ICM organoids and embryos immunostaining, and imaging

Primary antibodies include: NANOG (1:200, eBIOSCIENCE, 14-5761-80), OCT3/4 (1:200, SANTA CRUZ, SC5279), GATA6 (1:200, R&D, AF1700), SOX17 (1:200, R&D, AF1924), GATA4 (1:200, SANTA CRUZ, SC9053), Total β-catenin (1:500-1:1000, SIGMA, C2206), active β-catenin (1:300, MILLIPORE, 05-665), DUSP4 (1:100, Abcam, ab216576). Nuclei were visualized using Hoechst (Invitrogen, H3570) or DAPI (Invitrogen, D1306).

To visualise DUSP4, a tyramide signal amplification (TSA) reaction was carried out according to manufacturer's instructions (Invitrogen, B40943) and published protocol (Azami et al., 2019).

mESCs, ICM organoids and embryos were immunostained, and confocal imaged as previously described (Fischer et al., 2023; Mathew et al., 2019; Muñoz-Descalzo et al., 2013). To determine protein stabilities, mESCs were induced to differentiate to Epi- or PrE-like as previously published by adding Dox for 6h (Schroter et al., 2015). 24h after Dox removal, 40 μM cycloheximide was added to inhibit translation for 0h (control), 2h, 4h or 6h.

Confocal images were acquired using a Zeiss LSM-510-META with a Plan-Apochromat 63x/1.4 Oil Ph3 objective with 0.7x zoom, LSM-880 + Airyscan with a 40x/1.3 Oil DIC UV-IR M27 objective or Zeiss LSM700 and a Plan-Apochromat 40x/1.3 Oil DIC (UV) VIS-IR M27 objective laser scanning confocal microscopes.

Image and data analyses

Images and data were analysed as previously described (Fischer et al., 2023; Mathew et al., 2019; Muñoz-Descalzo et al., 2013) using MINS (Lou et al., 2014).

Exponential decay to estimate protein stability was modelled using Mathematica 11.0.

To quantify membrane β-catenin, ARIVIS software was used to help with visualization. ImageJ was used for quantification by drawing a line across the membrane between the indicated cells.

Data analyses were performed (Fischer et al., 2020; Fischer et al., 2023) using Paleontological Statistics (PAST) (Hammer et al., 2001), GraphPad Prism, Matlab R2017b, and Mathematica 11.0.

Statistical analysis

For the comparison of expression levels, Mann-Whitney tests were applied. Z-test was applied to compare populations. Bonferroni correction was applied when necessary.

Western blotting

Western blot was performed as previously published (Faunes et al., 2013). Briefly, cells were lysated with RIPA buffer supplemented with a protease inhibitor cocktail (PPC1010, Sigma-Aldrich), centrifuged 10000g for 10 min, quantify using a BCA assay and preserved frozen at -80°C. 120mg of total protein were loaded into a polyacrylamide gel. Anti GAPDH (1:5000, Sigma, 9545) was used as loading control.

scRNAseq data analyses

Mouse single-cell RNA-seq data is already published and may be accessed at https://brickman-preimplantation.streamlit.app/Download (file: 01_mouse_reprocessed.h5ad) (Linneberg-Agerholm et al., 2024). Plots were performed with Python (v3.12.3) using specific libraries such as Scanpy (v1.10.4), Seaborn (v0.13.2), Matplotlib (v3.8.4), NumPy (v1.26.4), Pandas (v1.5.3), and statannotations (0v.7.1). Jupyter code is available at Github: https://github.com/kuaiat/Jupyter.

Use of artificial intelligence tools

We utilized Copilot to assist in the refinement of the manuscript and ChatGPT for Python code assistance and debugging.

ACKNOWLEDGEMENTS

Lesley Moore in the Animal Facility at the University of Bath, Christian Schröter for the GATA6 inducible cells. Alfonso Martinez Arias and Kat Hadjantonakis during the very early stage of this work. Cristina Merino for help in the schemes shown in Fig S4B, C and F. Michael Eibl for annotating ICM chimeric organoids. Early work at the University of Bath was supported by a Wellcome Trust Seed Award (109589/Z/15/Z) and ECS funding was provided by the University of Bath. At the ULPGC, work at SMDlab was funded by the ACIISI (CEI2019-02), Programa de Ayudas a la Investigación de la ULPGC, and ACIISI co-funded by FEDER Funds (ProID2020010013). JLG was supported by the ULPGC predoctoral program and SMD was supported by the ‘‘Viera y Clavijo’’ Program from the ACIISI, and the ULPGC. Imaging at the IUIBS was done at the SIMACE (Servicio de Investigación en Microscopía Avanzada Confocal y Electrónica). Mouse work at the IUIBS was done at the now established SABiA (Servicio de Animalario y Bienestar Animal). TB was funded by a “Ayuda para Personal Técnico de Apoyo” from the Ministerio de Economía Industria y Competitividad (PTA2017-14230-I). Animal work at the ULPGC was done at the SABiA (Servicio Científico Servicio de Animalario y Bienestar Animal). Work at the SCF lab was supported through funding by the Deutsche Forschungsgemeinschaft (DFG, German Research Foundation) project number 470129398 and start-up funding by the University of Wuerzburg. MV funding was provided by EMBO Postdoctoral fellowships (ALTF 509-2015).

COMPETING INTERESTS

The authors declare no competing interests.

DATA AVAILABILITY

All data and information required to reanalyse the data reported in this paper is available from the corresponding author request.

AUTHOR CONTRIBUTIONS

SMD conceptualised this study with input from JLG. JLG, ECS, MV, TB and SMD performed experiments. JLG, SCF, JG and SMD analysed the data. SMD wrote the manuscript with input from JLG. All authors reviewed the final manuscript prior to submission.

DIVERSITY AND INCLUSION STATEMENT

We support inclusive, diverse, and equitable conduct of research.

REFERENCES

Anderson, K. G. V., Hamilton, W. B., Roske, F. V., Azad, A., Knudsen, T. E., Canham, M. A., Forrester, L. M. and Brickman, J. M. (2017). Insulin fine-tunes self-renewal pathways governing naive pluripotency and extra-embryonic endoderm. *Nat Cell Biol* **19**, 1164–1177.

Arekatla, G., Trenzinger, C., Reimann, A., Loeffler, D., Kull, T. and Schroeder, T. (2023). Optogenetic manipulation identifies the roles of ERK and AKT dynamics in controlling mouse embryonic stem cell exit from pluripotency. *Dev Cell* **58**, 1022-1036.e4.

Artus, J., Piliszek, A. and Hadjantonakis, A. K. (2011). The primitive endoderm lineage of the mouse blastocyst: Sequential transcription factor activation and regulation of differentiation by Sox17. *Dev Biol* **350**, 393–404.

Athanasouli, P., Balli, M., De Jaime-Soguero, A., Boel, A., Papanikolaou, S., van der Veer, B. K., Janiszewski, A., Vanhessche, T., Francis, A., El Laithy, Y., et al. (2023). The Wnt/TCF7L1 transcriptional repressor axis drives primitive endoderm formation by antagonizing naive and formative pluripotency. *Nature Communications 2023 14:1* **14**, 1–19.

Azami, T., Bassalert, C., Allègre, N., Valverde Estrella, L., Pouchin, P., Ema, M. and Chazaud, C. (2019). Regulation of the ERK signalling pathway in the developing mouse blastocyst. *Development* **146**, dev177139.

Barcroft, L. C., Offenberg, H., Thomsen, P. and Watson, A. J. (2003). Aquaporin proteins in murine trophectoderm mediate transepithelial water movements during cavitation. *Dev Biol* **256**, 342–354.

Biechele, S., Cockburn, K., Lanner, F., Cox, B. J. and Rossant, J. (2013). Porcn-dependent Wnt signaling is not required prior to mouse gastrulation. *Development* **140**, 2961–2971.

Brault, V., Moore, R., Kutsch, S., Ishibashi, M., Rowitch, D. H., McMahon, A. P., Sommer, L., Boussadia, O. and Kemler, R. (2001). Inactivation of the β-catenin gene by Wnt1-Cre-mediated deletion results in dramatic brain malformation and failure of craniofacial development. *Development* **128**, 1253–1264.

Caunt, C. J. and Keyse, S. M. (2013). Dual-specificity MAP kinase phosphatases (MKPs). *FEBS J* **280**, 489–504.

Chambers, I., Colby, D., Robertson, M., Nichols, J., Lee, S., Tweedie, S. and Smith, A. (2003). Functional expression cloning of Nanog, a pluripotency sustaining factor in embryonic stem cells. *Cell* **113**, 643–655.

Chazaud, C., Yamanaka, Y., Pawson, T. and Rossant, J. (2006). Early Lineage Segregation between Epiblast and Primitive Endoderm in Mouse Blastocysts through the Grb2-MAPK Pathway. *Dev Cell* **10**, 615–624.

de Vries, W. N. (2004). Maternal -catenin and E-cadherin in mouse development. *Development* **131**, 4435–4445.

De Vries, W. N., Binns, L. T., Fancher, K. S., Dean, J., Moore, R., Kemler, R. and Knowles, B. B. (2000). Expression of Cre Recombinase in Mouse Oocytes: A Means to Study Maternal Effect Genes. *genesis* 110–112.

Faunes, F., Hayward, P., Muñoz-Descalzo, S., Chatterjee, S. S., Balayo, T., Trott, J., Christoforou, A., Ferrer-Vaquer, A., Hadjantonakis, A.-K., Dasgupta, R., et al. (2013). A membrane-associated β-catenin/Oct4 complex correlates with ground-state pluripotency in mouse embryonic stem cells. *Development* **140**, 1171–83.

Fischer, S. C., Corujo-Simon, E., Lilao-Garzon, J., Stelzer, E. H. K. and Muñoz-Descalzo, S. (2020). The transition from local to global patterns governs the differentiation of mouse blastocysts. *PLoS One* **15**, e0233030.

Fischer, S. C., Schardt, S., Lilao-Garzón, J. and Muñoz-Descalzo, S. (2023). The salt-and-pepper pattern in mouse blastocysts is compatible with signaling beyond the nearest neighbors. *iScience* **26**, 108106.

Frankenberg, S., Gerbe, F., Bessonnard, S., Belville, C., Pouchin, P., Bardot, O. and Chazaud, C. (2011). Primitive Endoderm Differentiates via a Three-Step Mechanism Involving Nanog and RTK Signaling. *Dev Cell* **21**, 1005–1013.

Gattiglio, M., Protzek, M. and Schröter, C. (2023). Population-level antagonism between FGF and BMP signaling steers mesoderm differentiation in embryonic stem cells. *Biol Open* **12**,.

Geiselmann, A., Micouin, A., Vandormael-Pournin, S., Laville, V., Chervova, A., Mella, S., Navarro, P. and Cohen-Tannoudji, M. (2024). PI3K/AKT signaling controls ICM maturation and proper epiblast and primitive endoderm specification in mice. *Dev Cell* **0**,.

Guo, G., Huss, M., Tong, G. Q., Wang, C., Li Sun, L., Clarke, N. D. and Robson, P. (2010). Resolution of Cell Fate Decisions Revealed by Single-Cell Gene Expression Analysis from Zygote to Blastocyst. *Dev Cell* **18**, 675–685.

Haegel, H., Larue, L., Ohsugi, M., Fedorov, L., Herrenknecht, K. and Kemler, R. (1995). Lack of β-catenin affects mouse development at gastrulation. *Development* **121**, 3529–3537.

Hammer, D. A. T., Ryan, P. D., Hammer, Ø. and Harper, D. A. T. (2001). Past: Paleontological Statistics Software Package for Education and Data Analysis. *Palaeontologia Electronica* **4**, 178.

Hayashi, S., Lewis, P., Pevny, L. and McMahon, A. P. (2002). Efficient gene modulation in mouse epiblast using a Sox2Cre transgenic mouse strain. *Mech Dev* **119**, S97–S101.

Hou, Z., Wu, Q., Sun, X., Chen, H., Li, Y., Zhang, Y., Mori, M., Yang, Y., Que, J. and Jiang, M. (2019). Wnt/Fgf crosstalk is required for the specification of basal cells in the mouse trachea. *Development (Cambridge)* **146**,.

Huang, S.-M. M. A., Mishina, Y. M., Liu, S., Cheung, A., Stegmeier, F., Michaud, G. A., Charlat, O., Wiellette, E., Zhang, Y., Wiessner, S., et al. (2009). Tankyrase inhibition stabilizes axin and antagonizes Wnt signalling. *Nature* **461**, 614–620.

Kalkan, T., Olova, N., Roode, M., Mulas, C., Lee, H. J., Nett, I., Marks, H., Walker, R., Stunnenberg, H. G., Lilley, K. S., et al. (2017). Tracking the embryonic stem cell transition from ground state pluripotency. *Development* **144**,.

Kalkan, T., Bornelöv, S., Mulas, C., Diamanti, E., Lohoff, T., Ralser, M., Middelkamp, S., Lombard, P., Nichols, J. and Smith, A. (2019). Complementary Activity of ETV5, RBPJ, and TCF3 Drives Formative Transition from Naive Pluripotency. *Cell Stem Cell* **24**, 785-801.e7.

765 **Kang, M., Piliszek, A., Artus, J. and Hadjantonakis, A.-K.** (2013). FGF4 is required for lineage
766 restriction and salt-and-pepper distribution of primitive endoderm factors but not their initial
767 expression in the mouse. *Development* **140**, 267–279.

768 **Kang, M., Garg, V. and Hadjantonakis, A. K.** (2017). Lineage Establishment and Progression within
769 the Inner Cell Mass of the Mouse Blastocyst Requires FGFR1 and FGFR2. *Dev Cell* **41**, 496-
770 510.e5.

771 **Kim, S.-H., Kim, M. O., Cho, Y.-Y., Yao, K., Kim, D. J., Jeong, C.-H., Yu, D. H., Bae, K. B., Cho, E. J.,**
772 **Jung, S. K., et al.** (2014). ERK1 phosphorylates Nanog to regulate protein stability and stem cell
773 self-renewal. *Stem Cell Res* **13**, 1–11.

774 **Latham, K. E. and Howe, C. C.** (1991). SPARC synthesis in pre-implantation and early post-
775 implantation mouse embryos. *Rouxs Arch Dev Biol* **199**, 364–369.

776 **Le Bin, G. C., Muñoz-Descalzo, S., Kurowski, A., Leitch, H., Lou, X., Mansfield, W., Etienne-Dumeau,**
777 **C., Grabole, N., Mulas, C., Niwa, H., et al.** (2014). Oct4 is required for lineage priming in the
778 developing inner cell mass of the mouse blastocyst. *Development* **141**, 1001–1010.

779 **Lilao-Garzón, J., Brito-Casillas, Y., Quesada-Canales, O., Wägner, A. M. and Muñoz-Descalzo, S.**
780 (2023). Maternal age, obesity and hyperglycaemia are associated with a delay in
781 preimplantation embryo development in mouse. *Reproduction* **166**, 235–245.

782 **Linneberg-Agerholm, M., Sell, A. C., Redó-Riveiro, A., Perera, M., Proks, M., Knudsen, T. E., Barral,**
783 **A., Manzanares, M. and Brickman, J. M.** (2024). The primitive endoderm supports lineage
784 plasticity to enable regulative development. *Cell* **0**,.

785 **Lou, X., Kang, M., Xenopoulos, P., Muñoz-Descalzo, S. and Hadjantonakis, A. K.** (2014). A rapid and
786 efficient 2D/3D nuclear segmentation method for analysis of early mouse embryo and stem cell
787 image data. *Stem Cell Reports* **2**, 382–397.

788 **Mathew, B., Muñoz-Descalzo, S., Corujo-Simon, E., Schröter, C., Stelzer, E. H. K. and Fischer, S. C.**
789 (2019). Mouse ICM Organoids Reveal Three-Dimensional Cell Fate Clustering. *Biophys J* **116**,
790 127–141.

791 **Meng, Y., Moore, R., Tao, W., Smith, E. R., Tse, J. D., Caslini, C. and Xu, X. X.** (2018). GATA6
792 phosphorylation by Erk1/2 propels exit from pluripotency and commitment to primitive
793 endoderm. *Dev Biol* **436**, 55–65.

794 **Messerschmidt, D. M. and Kemler, R.** (2010). Nanog is required for primitive endoderm formation
795 through a non-cell autonomous mechanism. *Dev Biol* **344**, 129–137.

796 **Messerschmidt, D., de Vries, W. N., Lorthongpanich, C., Balu, S., Solter, D. and Knowles, B. B.**
797 (2016). B-Catenin-Mediated Adhesion Is Required for Successful Preimplantation Mouse
798 Embryo Development. *Development* **143**, 1993–1999.

799 **Moghe, P., Belousov, R., Ichikawa, T., Iwatani, C., Tsukiyama, T., Erzberger, A. and Hiiragi, T.**
800 (2025). Coupling of cell shape, matrix and tissue dynamics ensures embryonic patterning
801 robustness. *Nature Cell Biology 2025* 1–16.

802 **Molotkov, A., Mazot, P., Brewer, J. R., Cinalli, R. M. and Soriano, P.** (2017). Distinct Requirements
803 for FGFR1 and FGFR2 in Primitive Endoderm Development and Exit from Pluripotency. *Dev Cell*
804 **41**, 511-526.e4.

Muñoz-Descalzo, S., Rue, P., Faunes, F., Hayward, P., Jakt, L. M., Balayo, T., Garcia-Ojalvo, J. and Martinez Arias, A. (2013). A competitive protein interaction network buffers Oct4-mediated differentiation to promote pluripotency in embryonic stem cells. *Mol Syst Biol* **9**, 694–694.

Muñoz-Descalzo, S., Hadjantonakis, A.-K. K. and Arias, A. M. (2015). Wnt/ß-catenin signalling and the dynamics of fate decisions in early mouse embryos and embryonic stem (ES) cells. *Semin Cell Dev Biol* **47–48**, 101–109.

Nichols, J., Silva, J., Roode, M. and Smith, A. (2009). Suppression of Erk signalling promotes ground state pluripotency in the mouse embryo. *Development* **136**, 3215–3222.

Niwa, Y., Masamizu, Y., Liu, T., Nakayama, R., Deng, C. X. and Kageyama, R. (2007). The Initiation and Propagation of Hes7 Oscillation Are Cooperatively Regulated by Fgf and Notch Signaling in the Somite Segmentation Clock. *Dev Cell* **13**, 298–304.

Nowotschin, S., Setty, M., Kuo, Y. Y., Liu, V., Garg, V., Sharma, R., Simon, C. S., Saiz, N., Gardner, R., Boutet, S. C., et al. (2019). The emergent landscape of the mouse gut endoderm at single-cell resolution. *Nature* **569**, 361–367.

Ohnishi, Y., Huber, W., Tsumura, A., Kang, M., Xenopoulos, P., Kurimoto, K., Oleś, A. K., Araúzo-Bravo, M. J., Saitou, M., Hadjantonakis, A.-K., et al. (2013). Cell-to-cell expression variability followed by signal reinforcement progressively segregates early mouse lineages. *Nat Cell Biol* **16**, 27–37.

Perera, M. and Brickman, J. M. (2024). Common modes of ERK induction resolve into context-specific signalling via emergent networks and cell-type-specific transcriptional repression. *Development* **151**,.

Plusa, B., Piliszek, A., Frankenberg, S., Artus, J. and Hadjantonakis, A.-K. (2008). Distinct sequential cell behaviours direct primitive endoderm formation in the mouse blastocyst. *Development* **135**, 3081–3091.

Pokrass, M. J., Ryan, K. A., Xin, T., Pielstick, B., Timp, W., Greco, V. and Regot, S. (2020). Cell-Cycle-Dependent ERK Signaling Dynamics Direct Fate Specification in the Mammalian Preimplantation Embryo. *Dev Cell*.

Raina, D., Fabris, F., Morelli, L. G. and Schröter, C. (2022). Intermittent ERK oscillations downstream of FGF in mouse embryonic stem cells. *Development (Cambridge)* **149**,.

Richard, C., Gao, J., Brown, N. and Reese, J. (2003). Aquaporin Water Channel Genes Are Differentially Expressed and Regulated by Ovarian Steroids during the Periimplantation Period in the Mouse. *Endocrinology* **144**, 1533–1541.

Saiz, N., Williams, K. M., Seshan, V. E. and Hadjantonakis, A.-K. (2016). Asynchronous fate decisions by single cells collectively ensure consistent lineage composition in the mouse blastocyst. *Nat Commun* **7**, 13463.

Saiz, N., Mora-Bitria, L., Rahman, S., George, H., Herder, J., Garcia-Ojalvo, J. and Hadjantonakis, A.-K. (2020). Growth factor-mediated coupling between lineage size and cell fate choice underlies robustness of mammalian development. *Elife* **9**,.

Schrode, N., Saiz, N., Di Talia, S. and Hadjantonakis, A.-K. (2015). GATA6 Levels Modulate Primitive Endoderm Cell Fate Choice and Timing in the Mouse Blastocyst. *Nih* **29**,.

Schroter, C., Rue, P., Mackenzie, J. P. and Martinez Arias, A. (2015). FGF/MAPK signaling sets the switching threshold of a bistable circuit controlling cell fate decisions in embryonic stem cells. *Development* **142**, 4205–4216.

Simon, C. S., Rahman, S., Raina, D., Schröter, C. and Hadjantonakis, A.-K. (2020). Live Visualization of ERK Activity in the Mouse Blastocyst Reveals Lineage-Specific Signaling Dynamics. *Dev Cell* **0**,.

Singh, A. M., Hamazaki, T., Hankowski, K. E. and Terada, N. (2007). A Heterogeneous Expression Pattern for Nanog in Embryonic Stem Cells. *Stem Cells* **25**, 2534–2542.

Smith, A. (2017). Formative pluripotency: the executive phase in a developmental continuum. *Development* **144**, 365–373.

Soszyńska, A., Klimczewska, K. and Suwińska, A. (2019). FGF/ERK signaling pathway: how it operates in mammalian preimplantation embryos and embryo-derived stem cells. *Int J Dev Biol* **63**, 171–186.

Thamodaran, V. and Bruce, A. W. (2016). p38 (Mapk14/11) occupies a regulatory node governing entry into primitive endoderm differentiation during preimplantation mouse embryo development. *Open Biol* **6**,.

Thompson, J. J., Lee, D. J., Mitra, A., Frail, S., Dale, R. K. and Rocha, P. P. (2022). Extensive co-binding and rapid redistribution of NANOG and GATA6 during emergence of divergent lineages. *Nature Communications 2022 13:1* **13**, 1–18.

Turner, D. A., Hayward, P. C., Baillie-Johnson, P., Rue, P., Broome, R., Faunes, F. and Martinez Arias, A. (2014). Wnt/ -catenin and FGF signalling direct the specification and maintenance of a neuromesodermal axial progenitor in ensembles of mouse embryonic stem cells. *Development* **141**, 4243–4253.

Wamaitha, S. E., del Valle, I., Cho, L. T. Y., Wei, Y., Fogarty, N. M. E., Blakeley, P., Sherwood, R. I., Ji, H. and Niakan, K. K. (2015). Gata6 potently initiates reprograming of pluripotent and differentiated cells to extraembryonic endoderm stem cells. *Genes Dev* **29**, 1239–1255.

White, M. D. and Plachta, N. (2019). Specification of the First Mammalian Cell Lineages In Vivo and In Vitro. *Cold Spring Harb Perspect Biol* a035634.

Wray, J., Kalkan, T., Gomez-Lopez, S., Eckardt, D., Cook, A., Kemler, R. and Smith, A. (2011). Inhibition of glycogen synthase kinase-3 alleviates Tcf3 repression of the pluripotency network and increases embryonic stem cell resistance to differentiation. *Nat Cell Biol* **13**, 838–845.

Xenopoulos, P., Kang, M., Puliafito, A., DiTalia, S. and Hadjantonakis, A. K. (2015). Heterogeneities in nanog expression drive stable commitment to pluripotency in the mouse blastocyst. *Cell Rep* **10**, 1508–01520.

Xie, H., Tranguch, S., Jia, X., Zhang, H., Das, S. K., Dey, S. K., Kuo, C. J. and Wang, H. (2008). Inactivation of nuclear Wnt- -catenin signaling limits blastocyst competency for implantation. *Development* **135**, 717–727.

Yanagida, A., Corujo-Simon, E., Revell, C. K., Sahu, P., Stirparo, G. G., Aspalter, I. M., Winkel, A. K., Peters, R., Belly, H. De, Cassani, D. A. D., et al. (2022). Cell surface fluctuations regulate early embryonic lineage sorting. *Cell* **0**, 1–17.

884 **Ying, Q.-L., Wray, J., Nichols, J., Batlle-Morera, L., Doble, B., Woodgett, J., Cohen, P. and Smith, A.**
885 (2008). The ground state of embryonic stem cell self-renewal. *Nature* **453**, 519–523.

886 **Zhang, X., Peterson, K. A., Liu, X. S., Mcmahon, A. P. and Ohba, S.** (2013). Gene regulatory networks
887 mediating canonical wnt signal-directed control of pluripotency and differentiation in embryo
888 stem cells. *Stem Cells* **31**, 2667–2679.

889

Figure 1: β-catenin localises in cell membranes in mouse preimplantation embryos

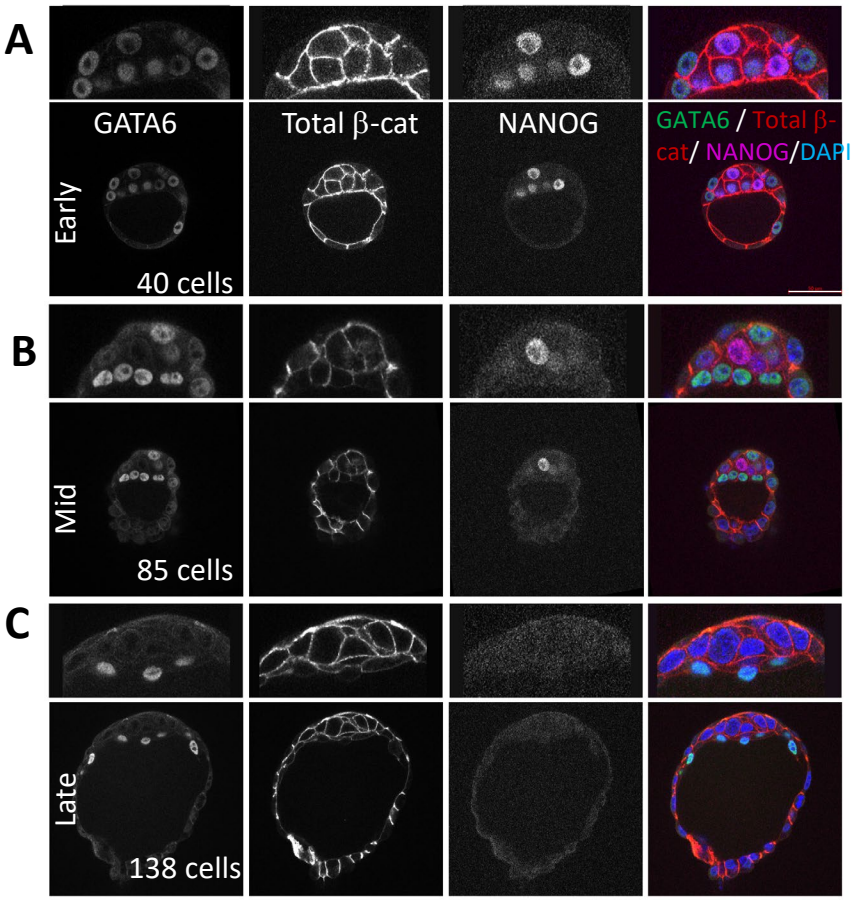

Figure 2: Membrane β-catenin quantification during cell fate acquisition

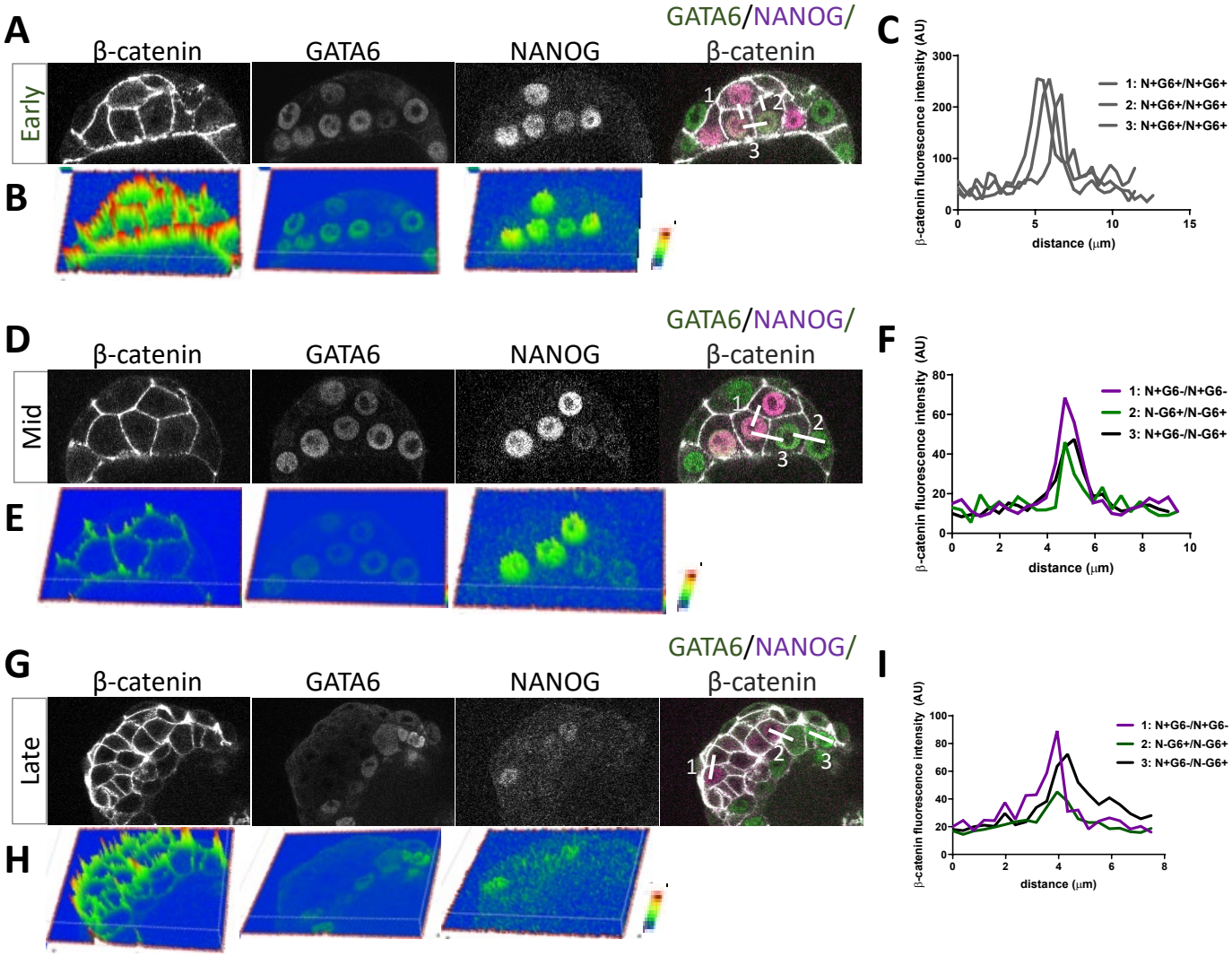

Figure 3: Chemical Wnt/β-catenin signalling modulation influences PrE fate *in vitro*

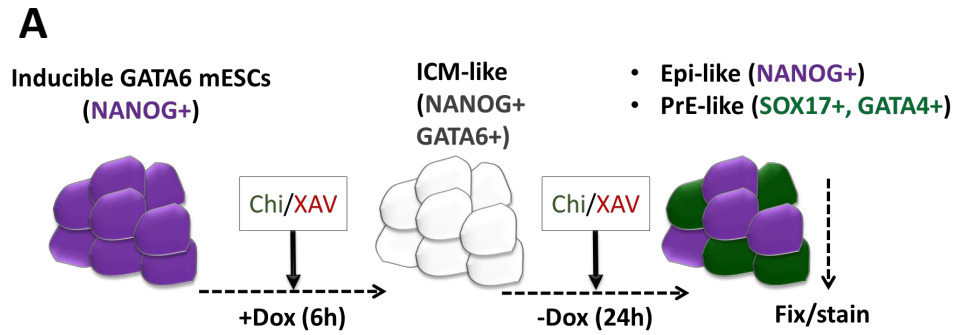

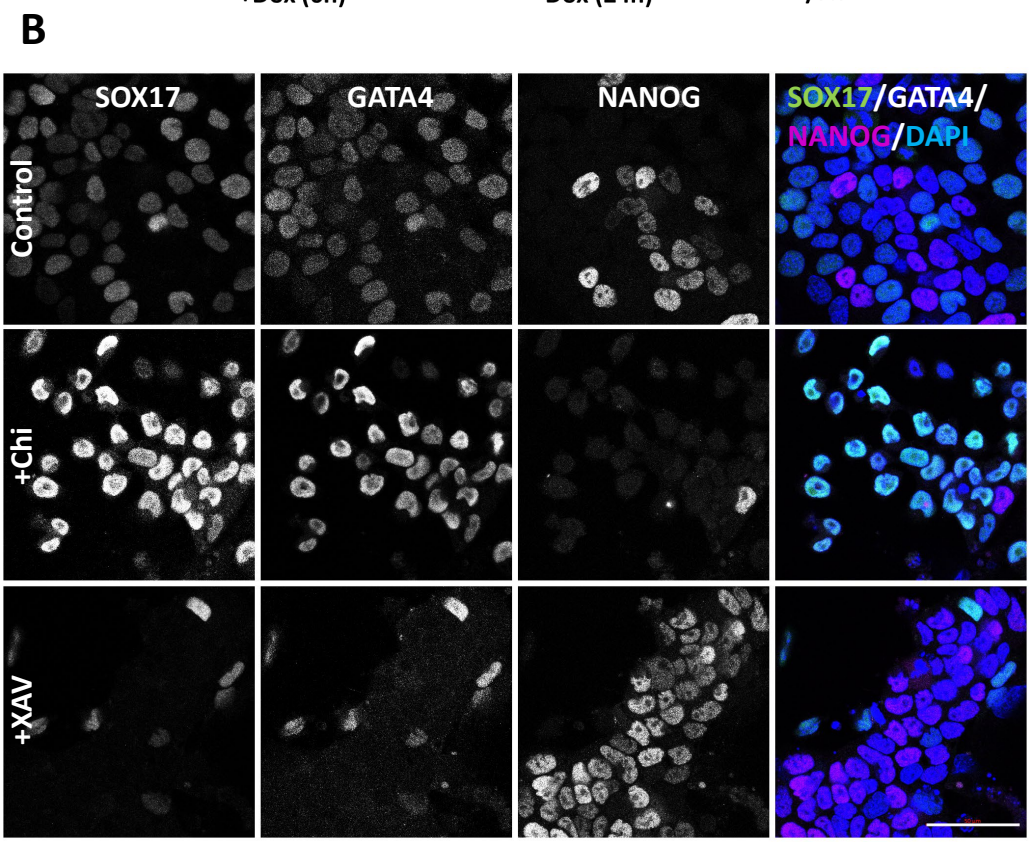

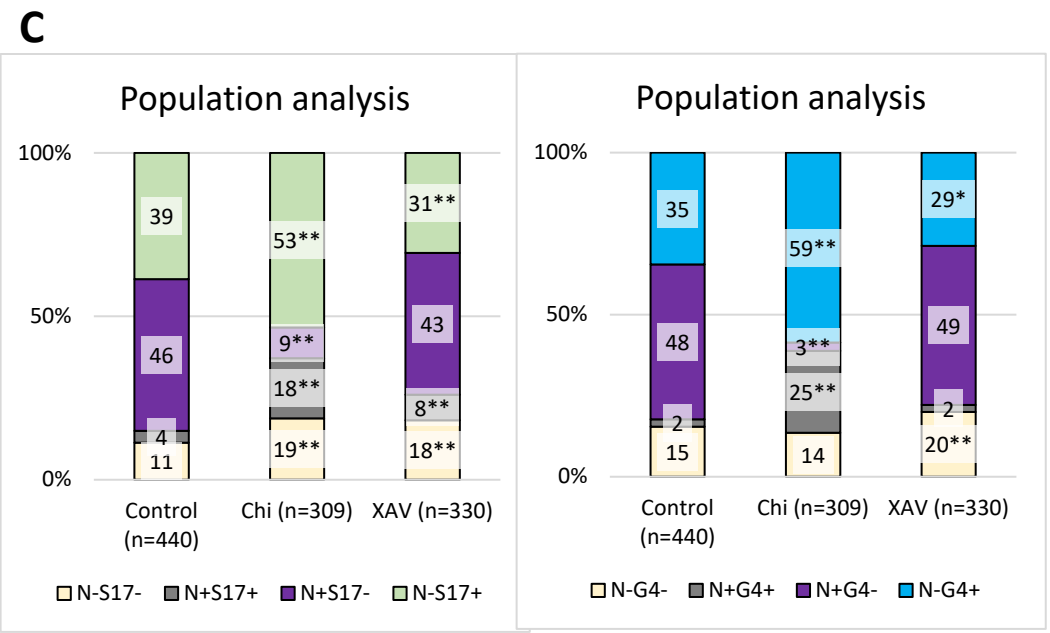

Figure 4: Chemical Wnt/β-catenin signalling modulation influences PrE fate *in vivo*

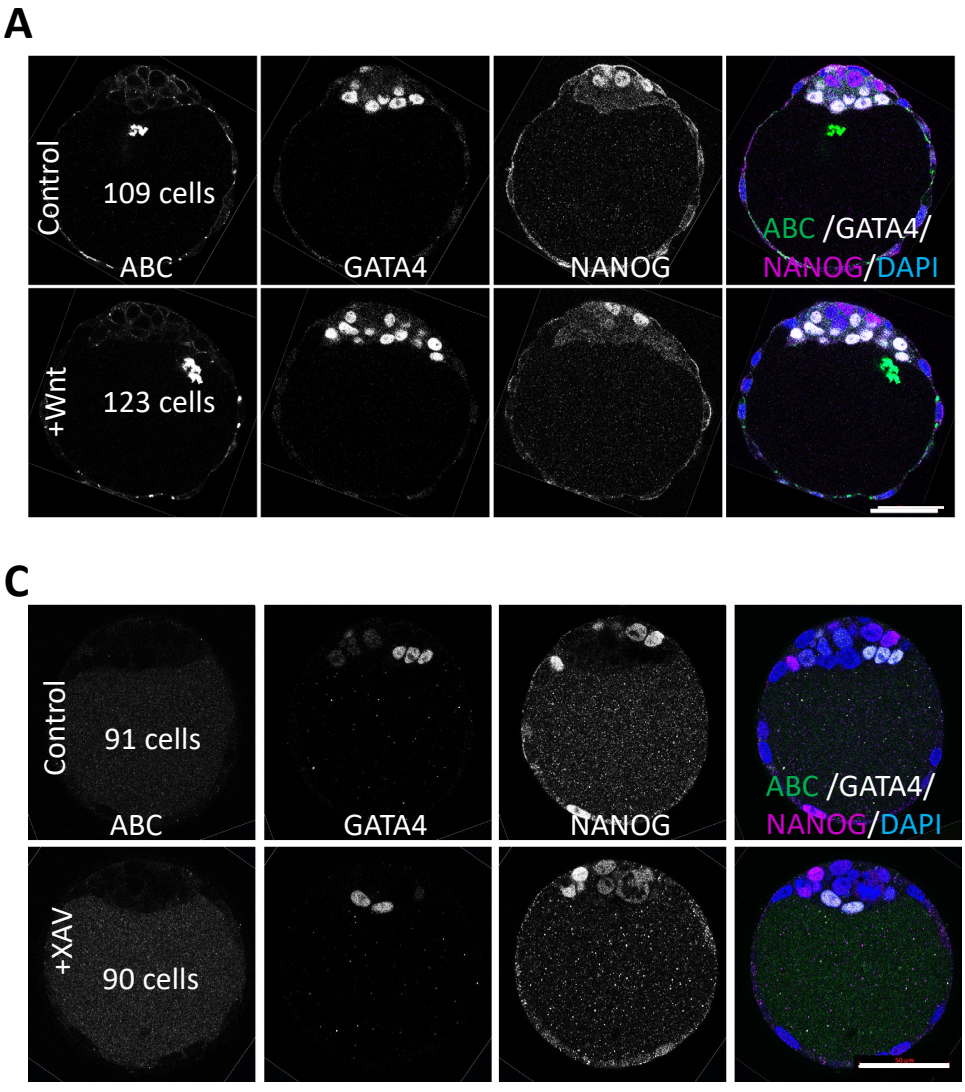

Figure 5: Genetic Wnt/β-catenin signalling inhibition hinders PrE fate *in vitro* (2D)

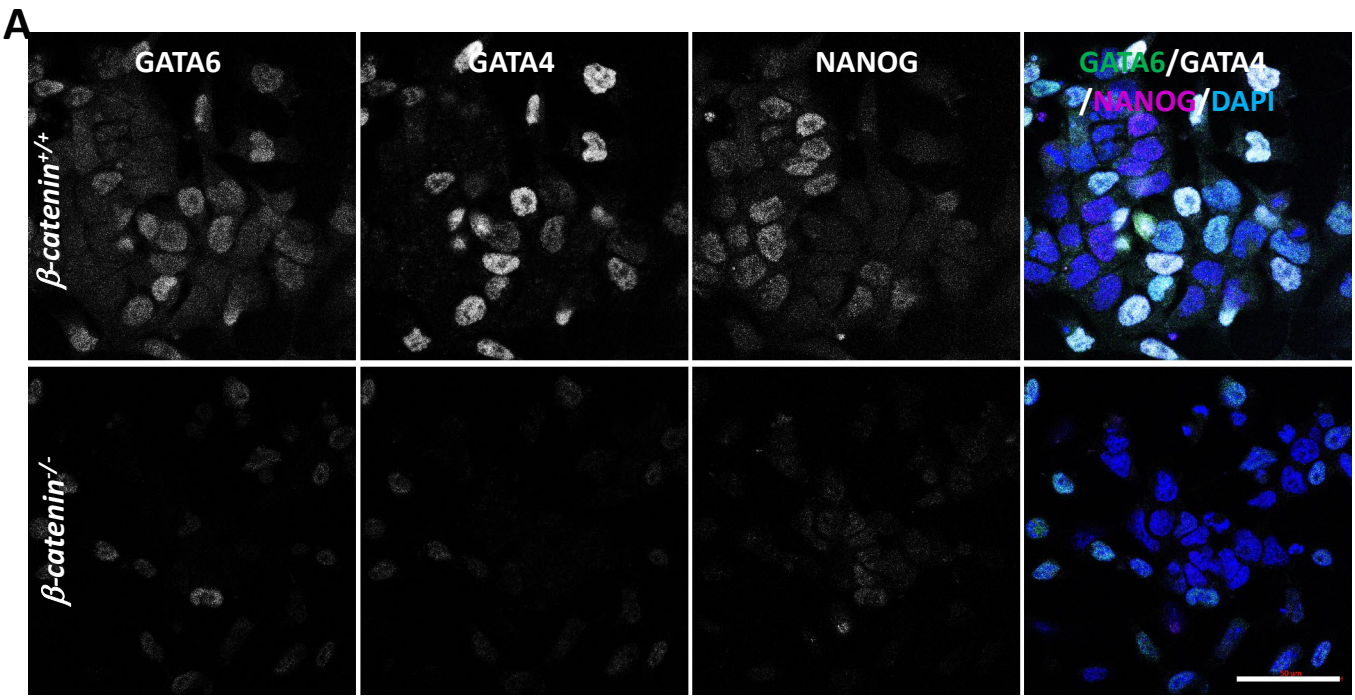

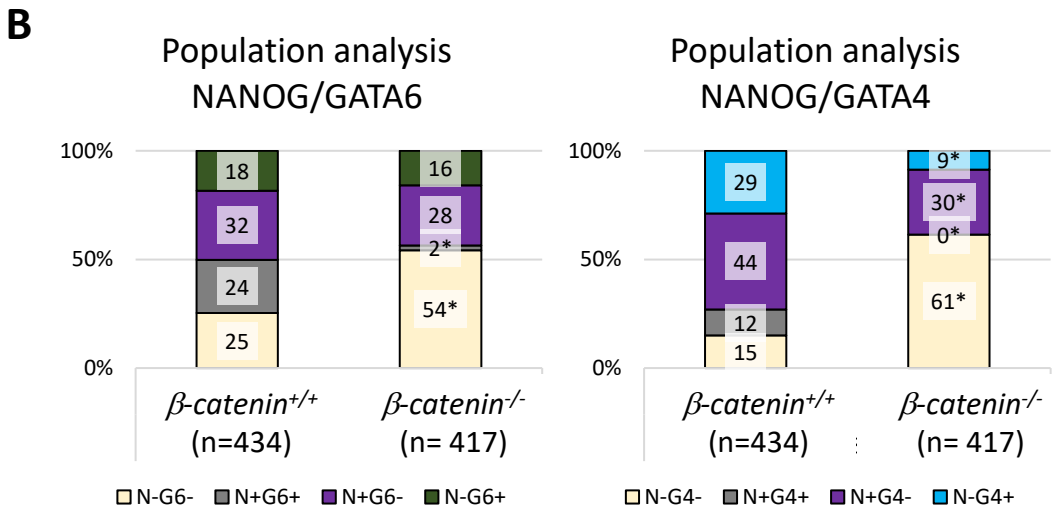

Figure 6: Genetic Wnt/β-catenin signalling inhibition hinders PrE fate *in vitro* (3D)

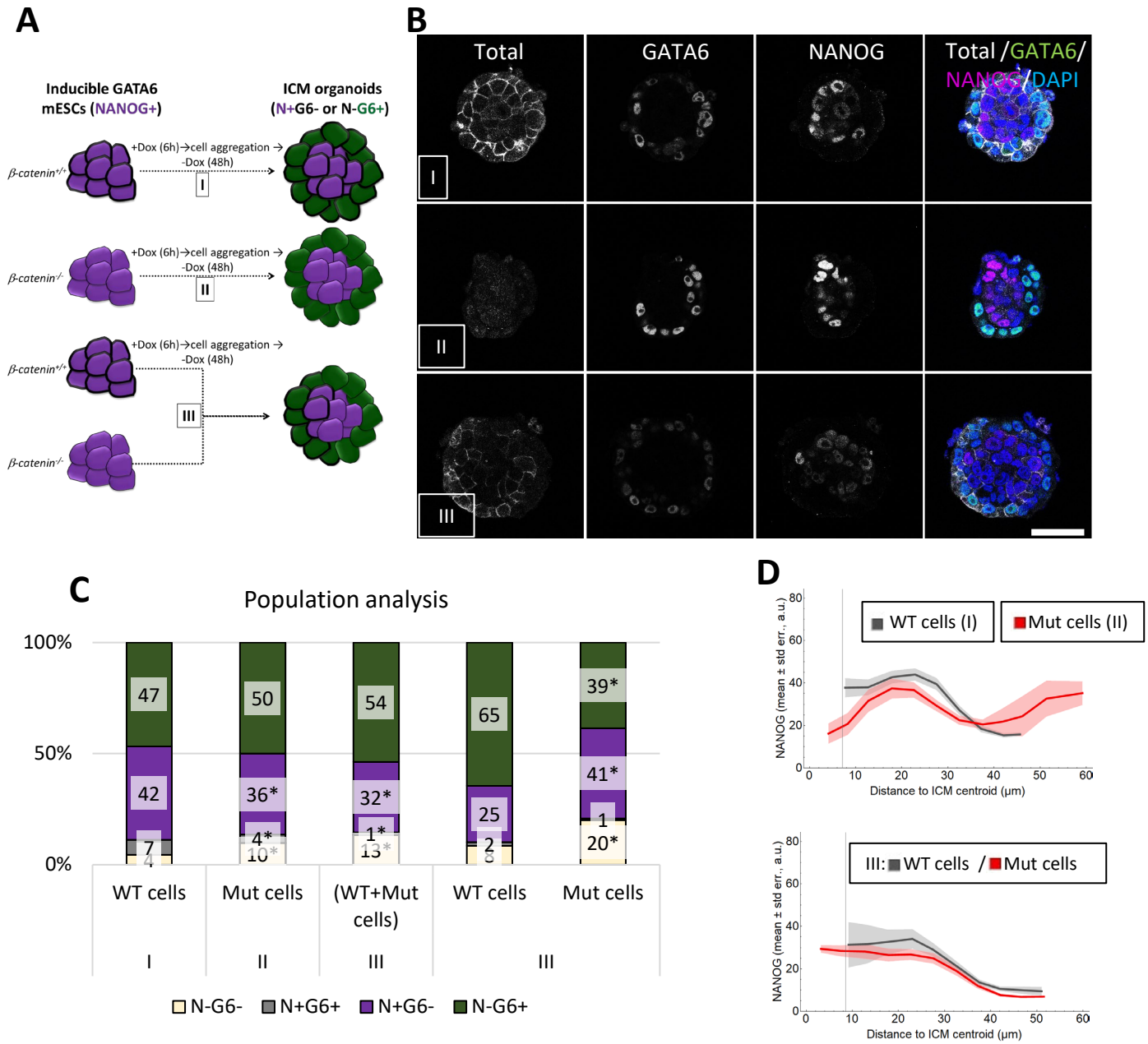

Figure 7: Genetic Wnt/β-catenin signalling inhibition hinders PrE fate *in vivo*

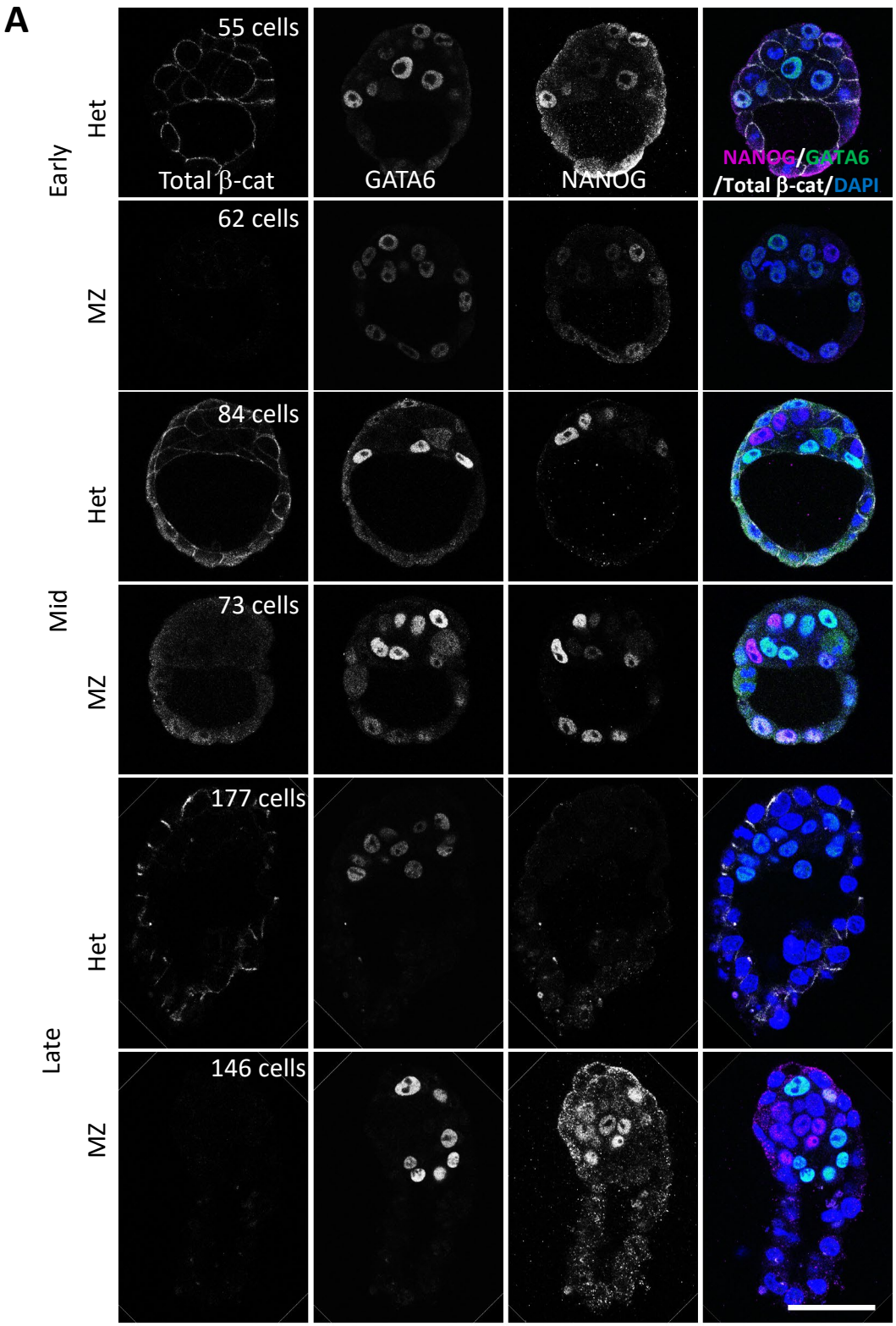

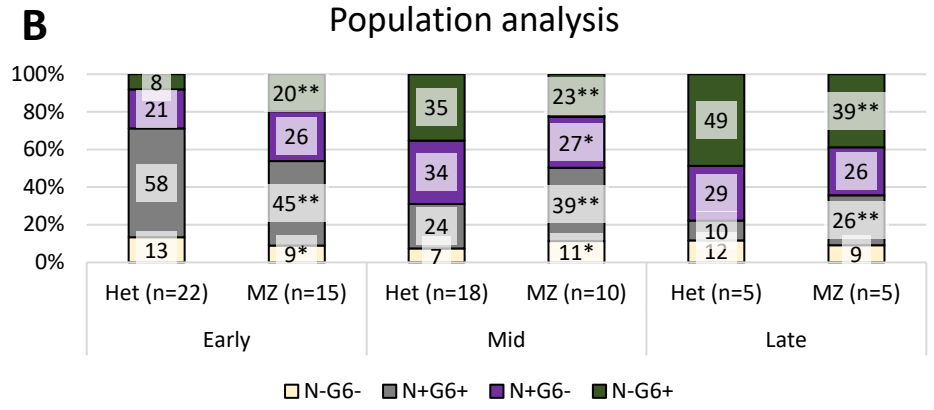

Figure 8: Wnt/β-catenin signalling cooperates with FGF/MAPK signalling in cell fate decisions in early mouse embryos

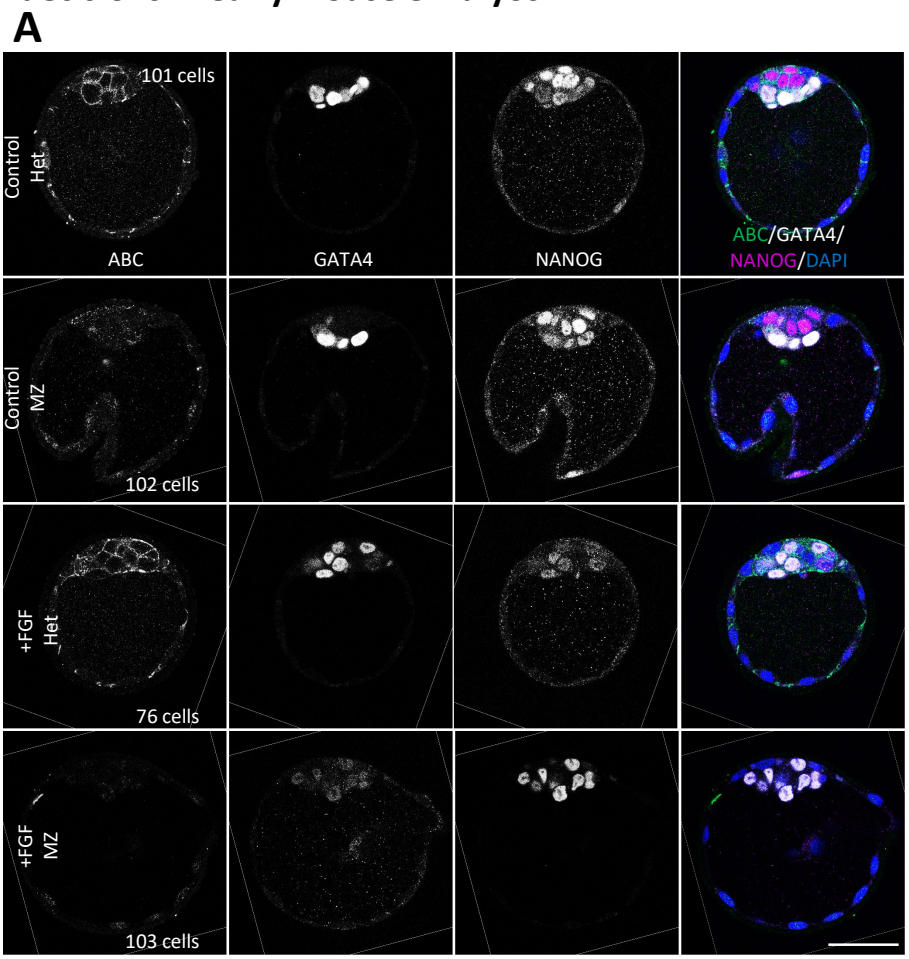

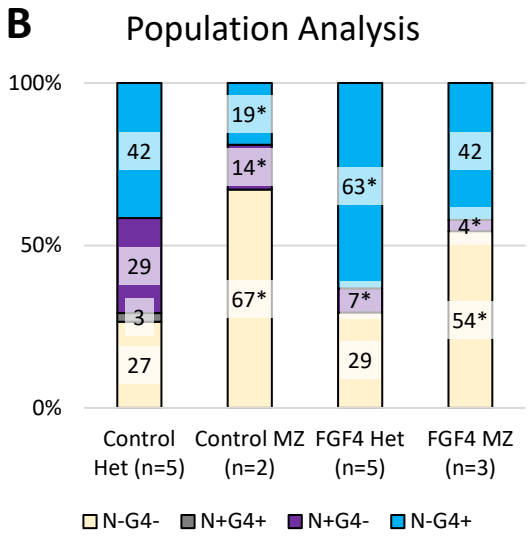

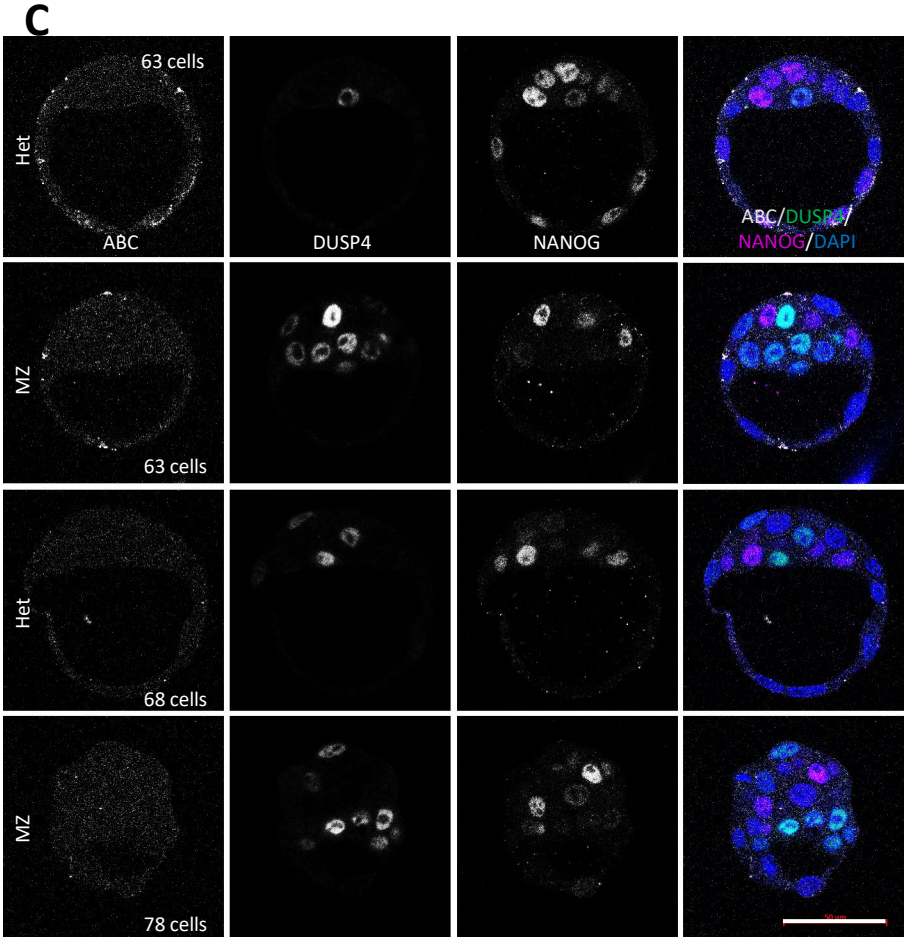

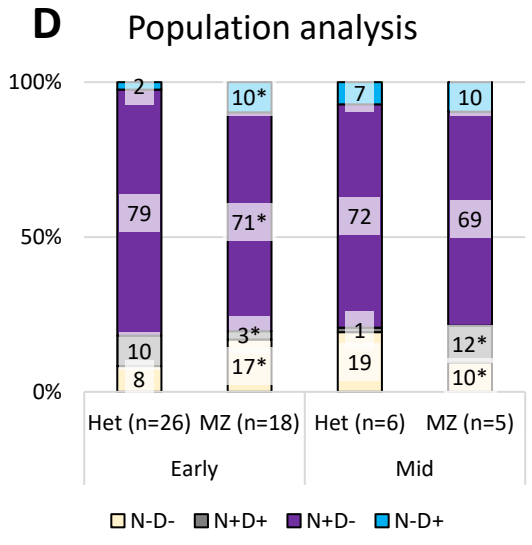

Figure 9: β-catenin acts independently of Wnt signalling activation during PrE differentiation via GATA6 and GATA4 turnover regulation

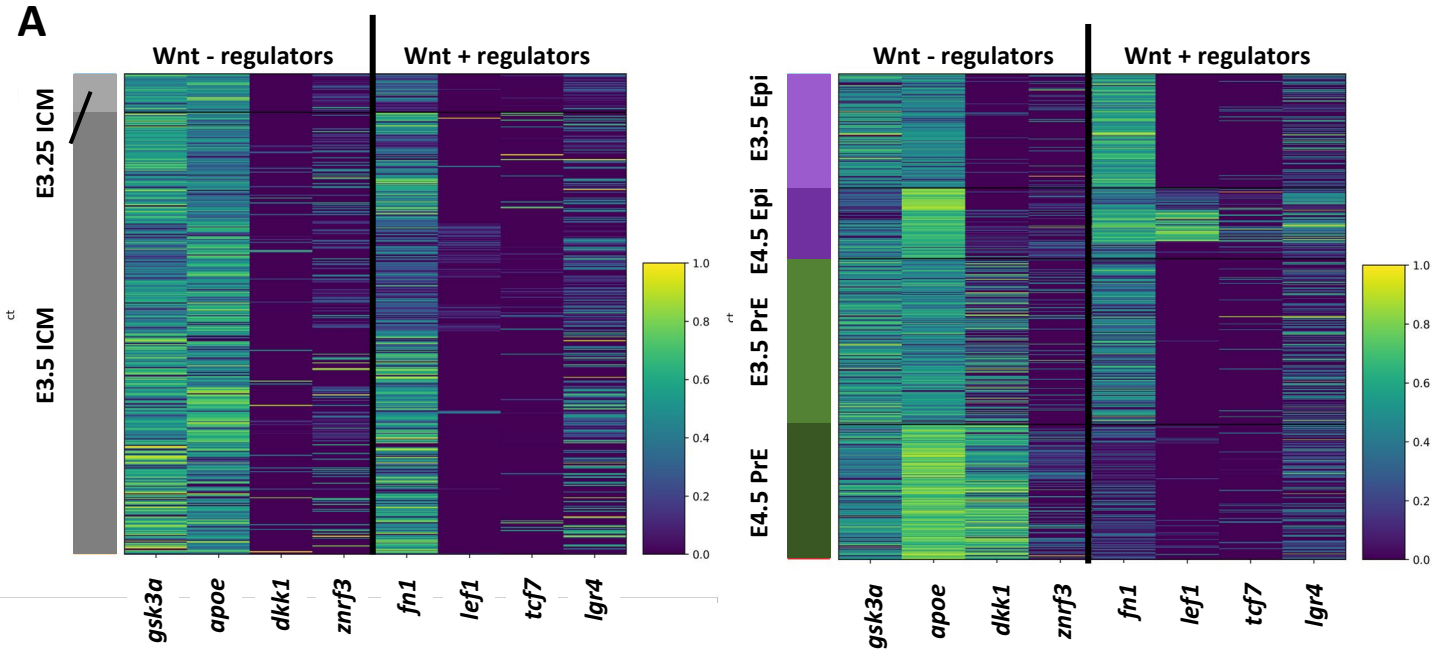

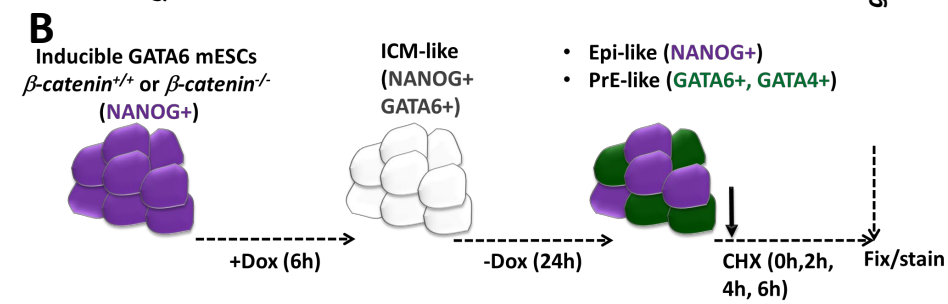

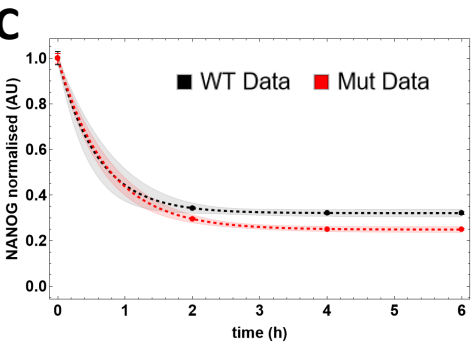

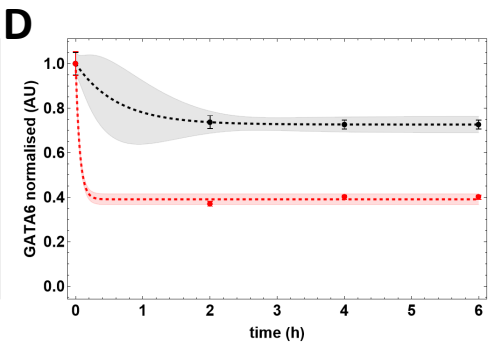

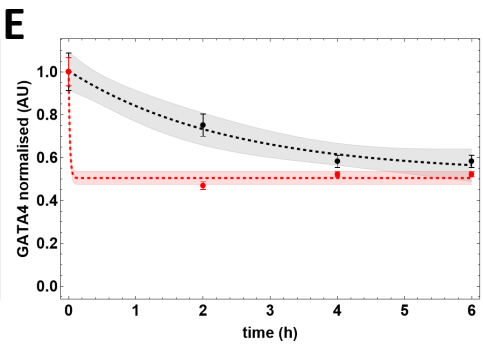

Figure 10: Working model for Wnt/β-catenin role during early mouse preimplantation embryo cell fate decision.

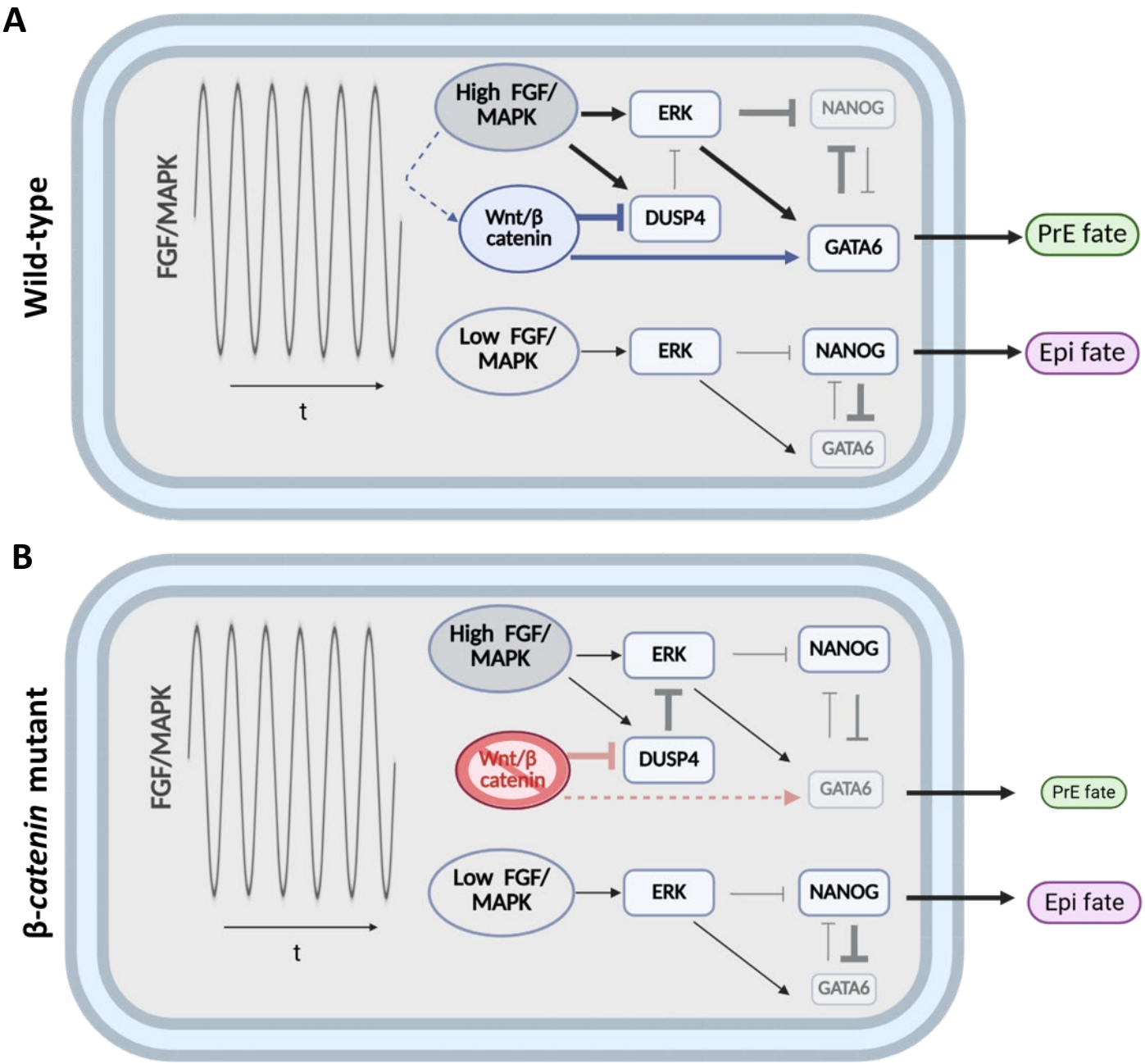

Figure S1: Active β-catenin localises in cell membranes in mouse preimplantation embryos

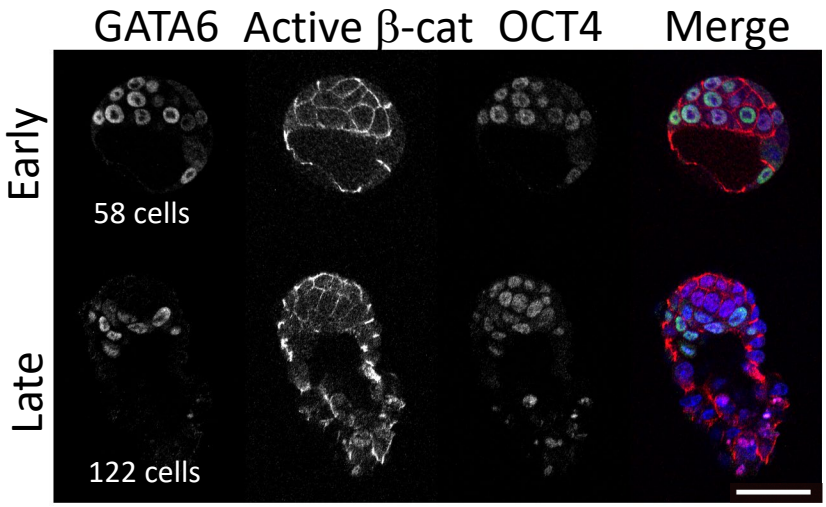

Figure S2: Chemical Wnt/β-catenin signalling modulation influences PrE fate *in vitro*

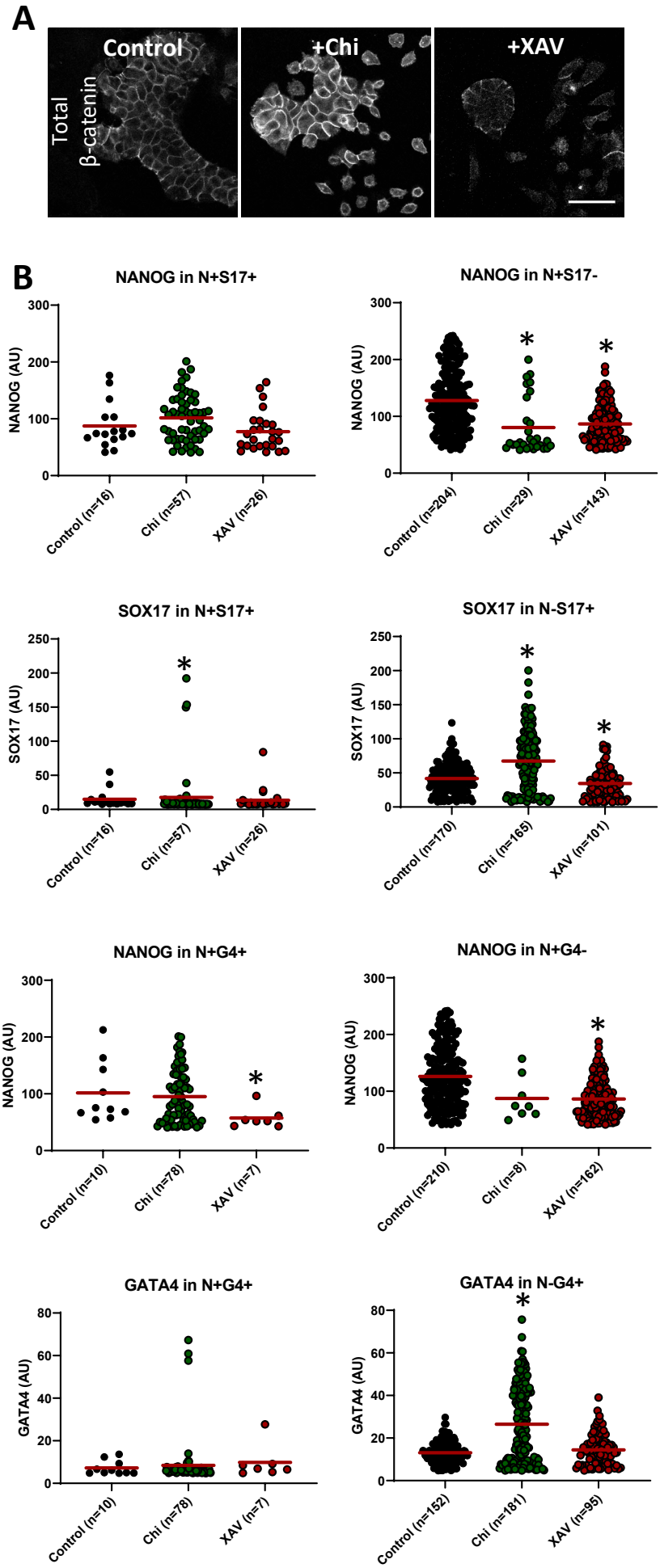

Figure S3: Chemical Wnt/β-catenin signalling activation promotes PrE fate *in vitro*

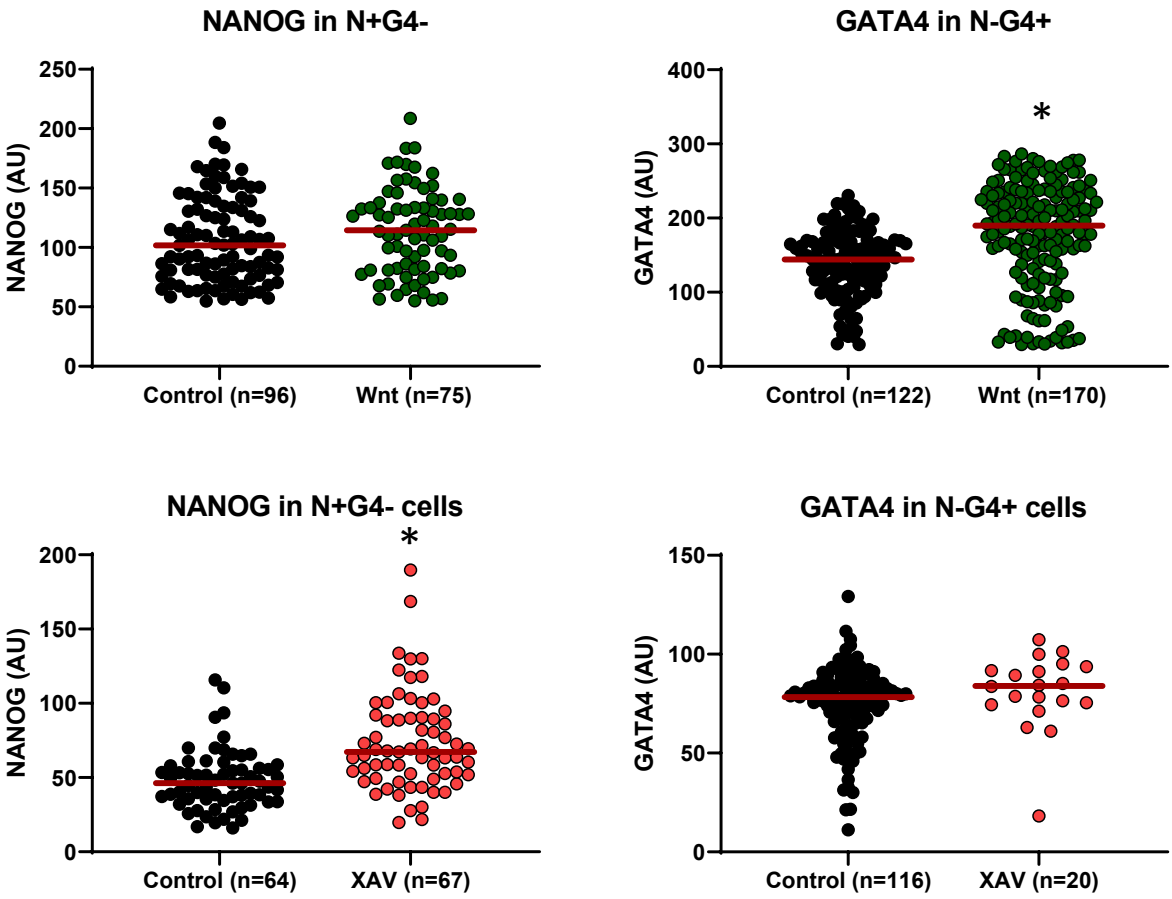

Figure S4: *β-catenin$^{-/-}$ tet::Gata6*-mCherry mESCs characterisation

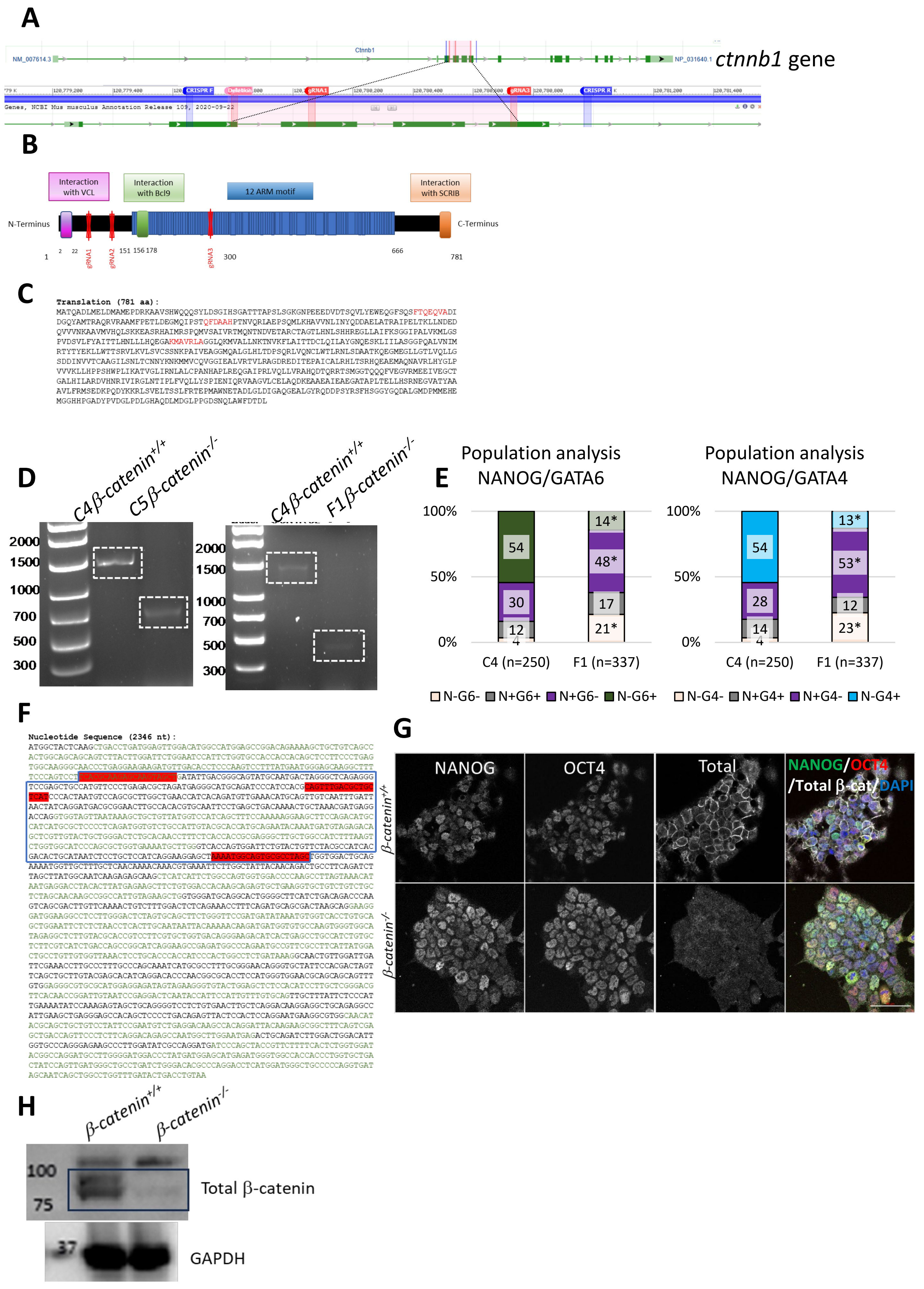

Figure S5: Genetic Wnt/β-catenin signalling inhibition hinders PrE fate *in vitro* (2D)

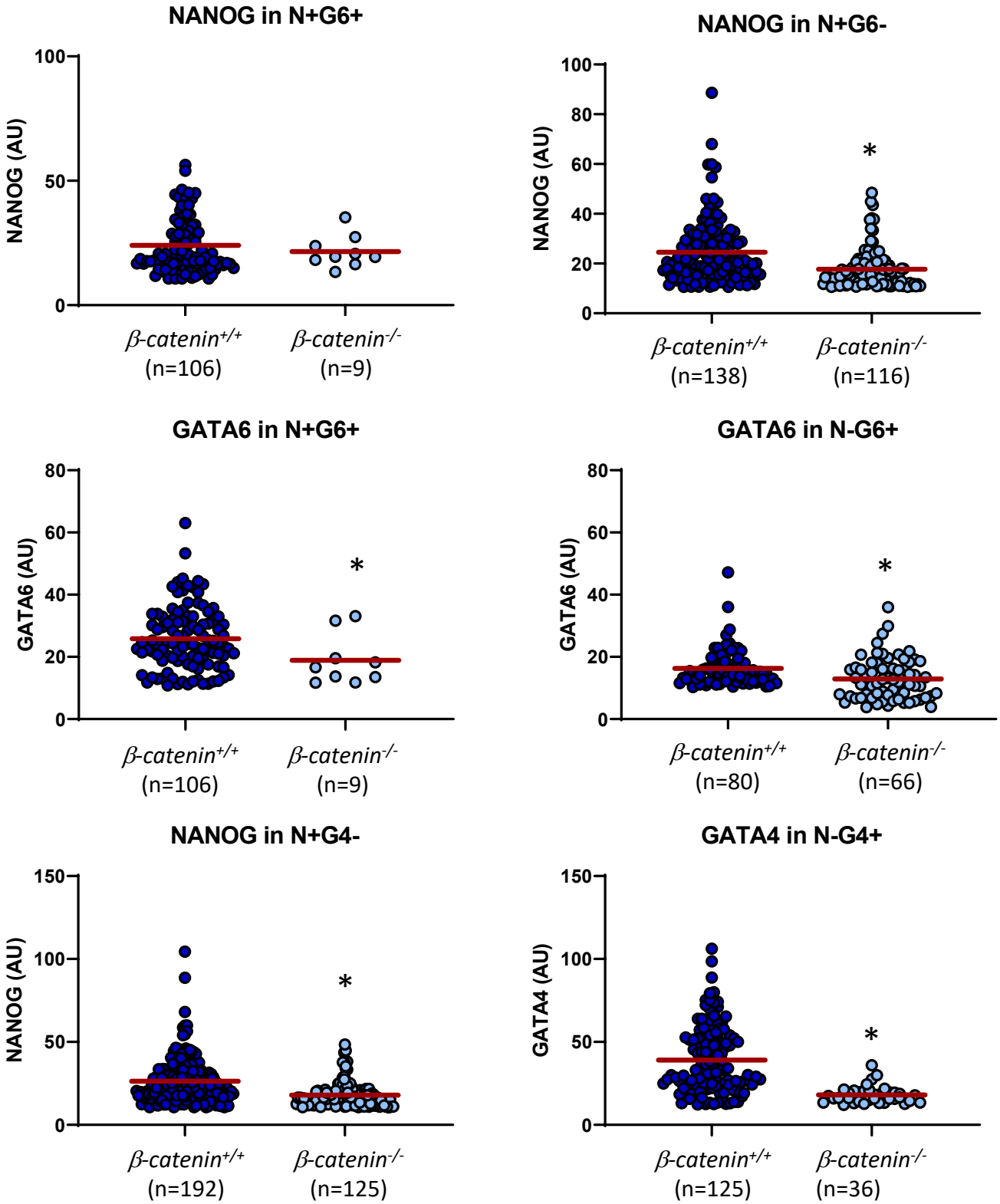

Figure S6: Genetic Wnt/β-catenin signalling inhibition hinders PrE fate *in vitro* (3D)

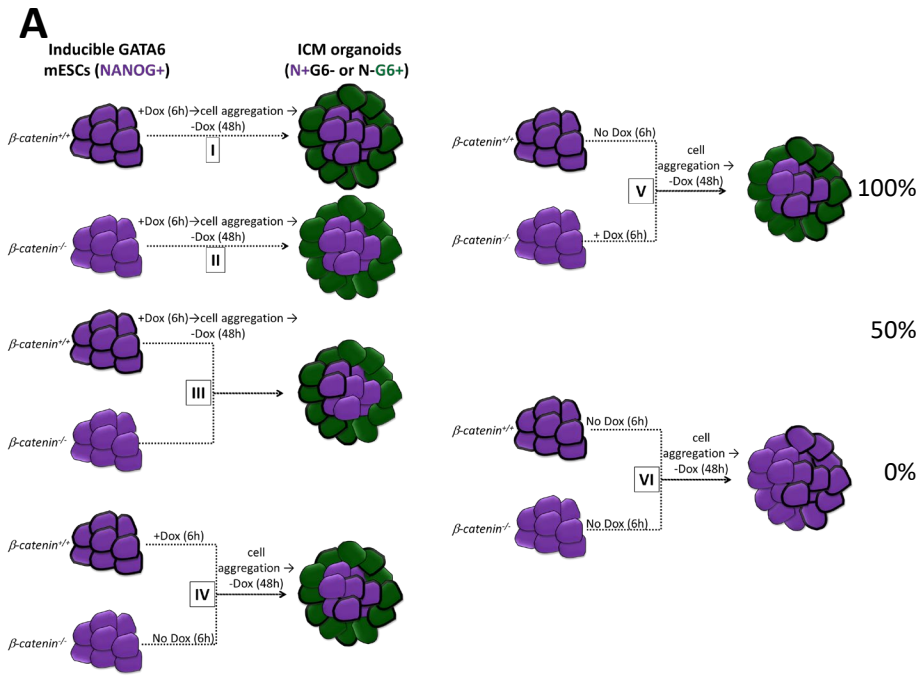

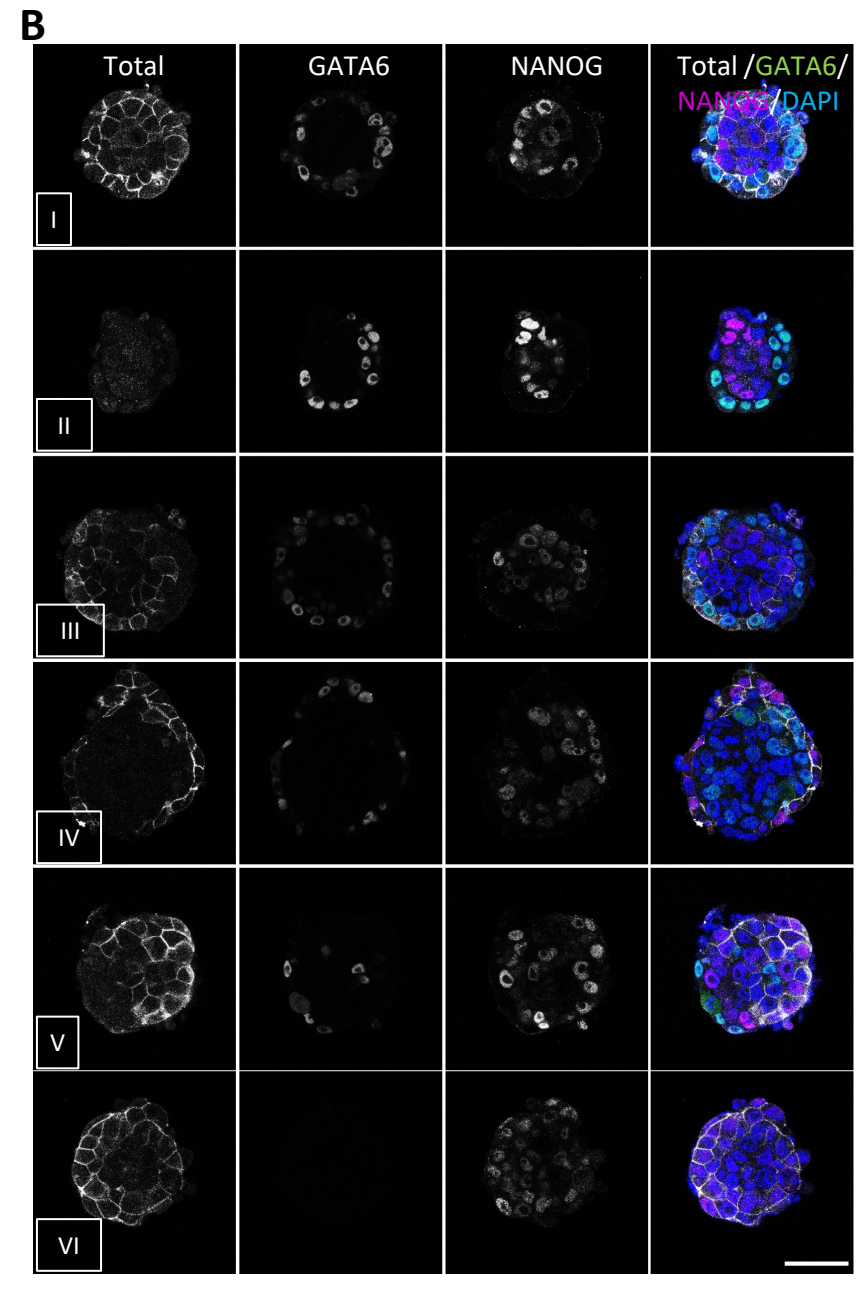

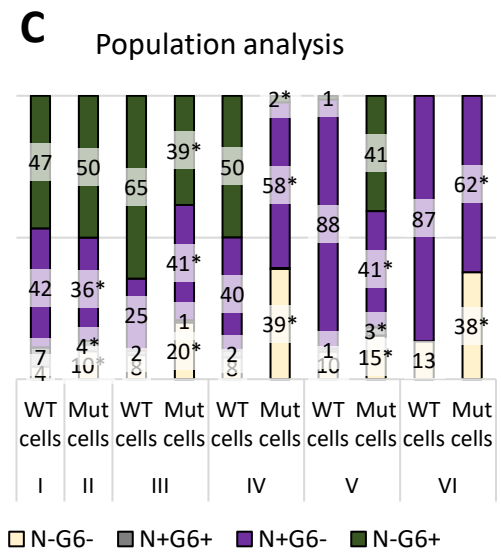

Figure S7: Genetic Wnt/β-catenin signalling inhibition hinders PrE fate *in vitro* (3D)

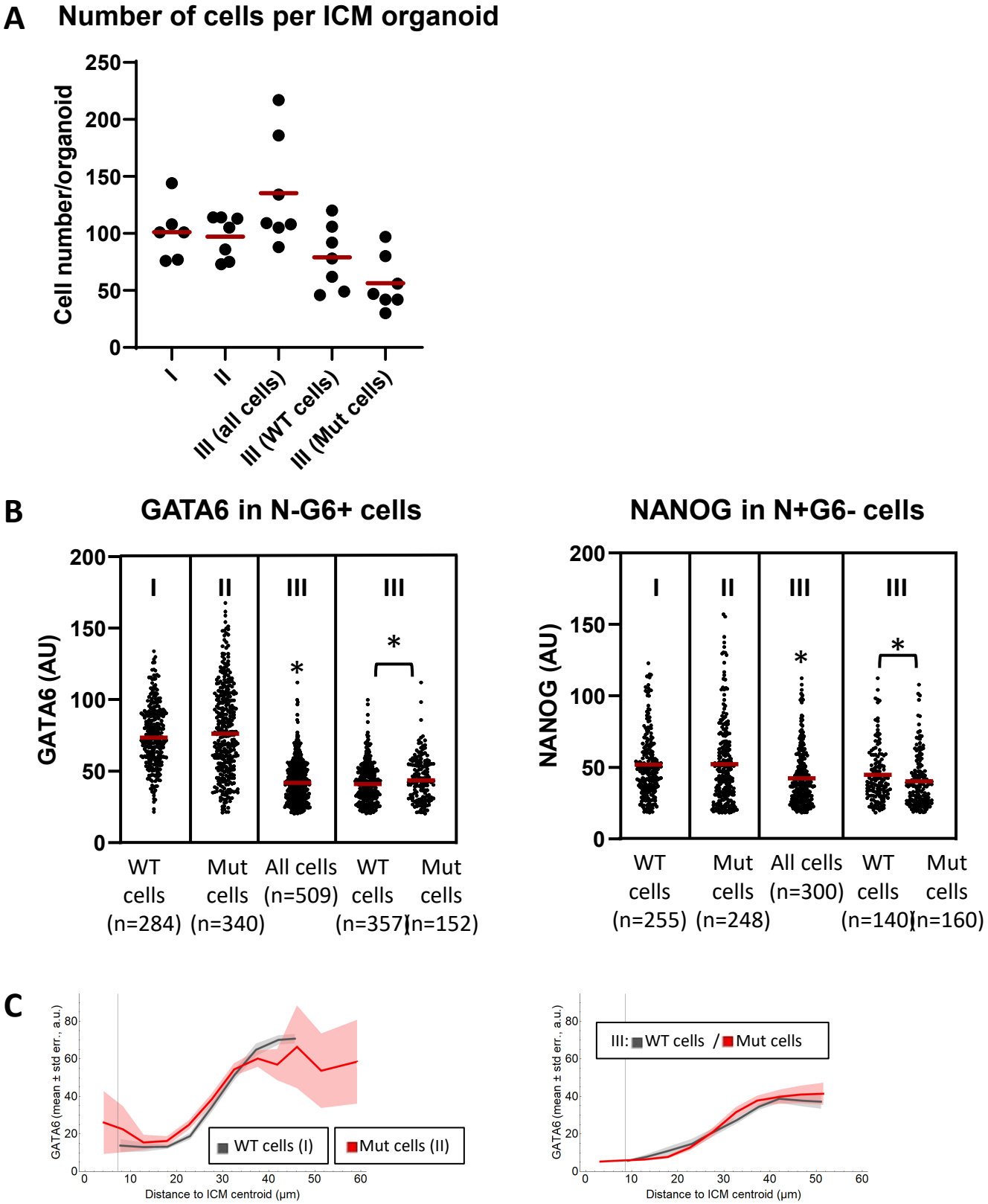

Figure S8: Genetic Wnt/β-catenin signalling inhibition hinders PrE fate *in vivo*

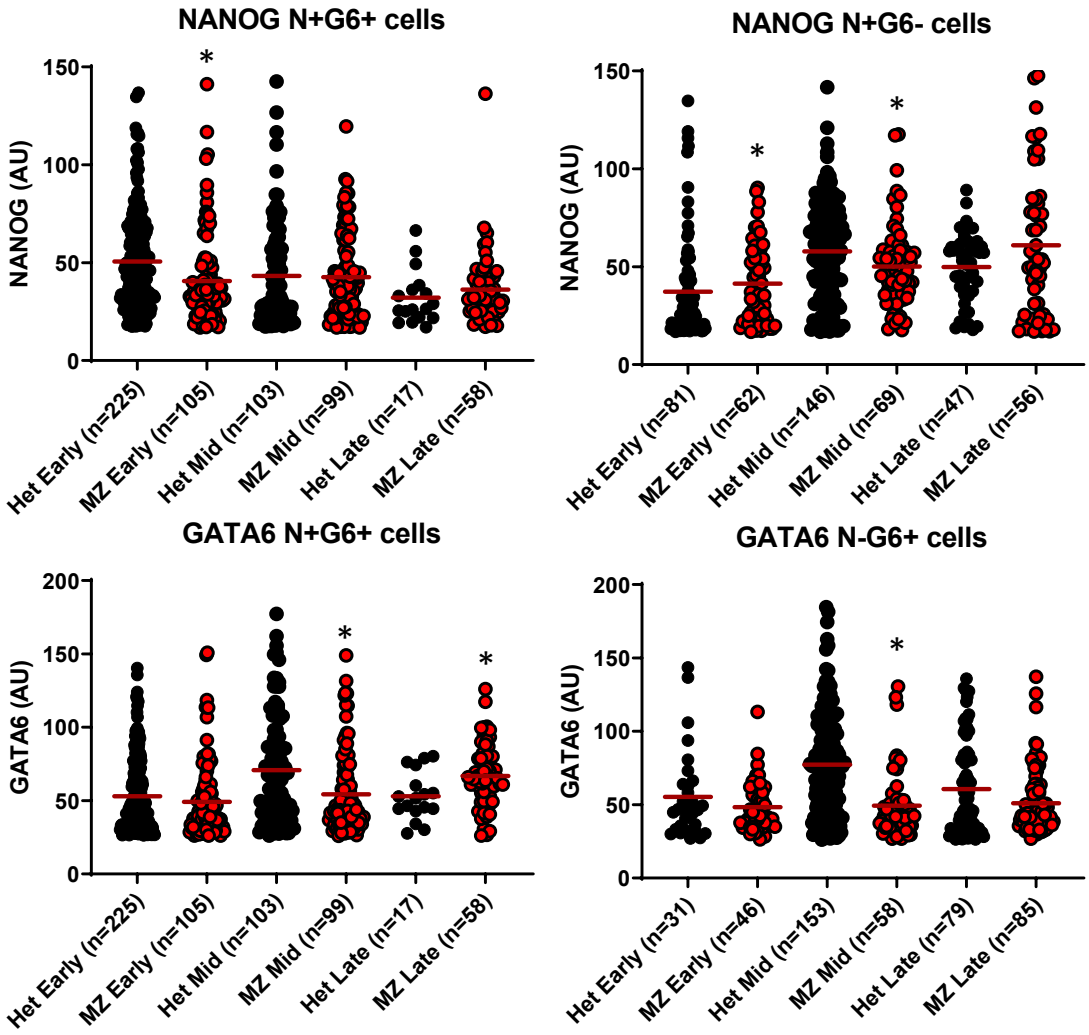

Figure S9: Wnt/β-catenin signalling cooperates with FGF/MAPK signalling in cell fate decisions in early mouse embryos

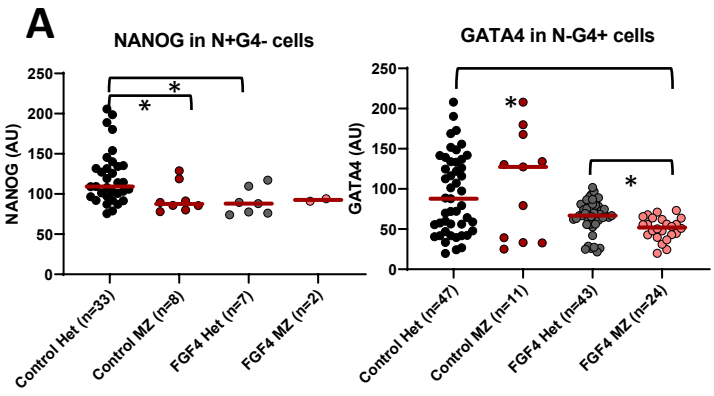

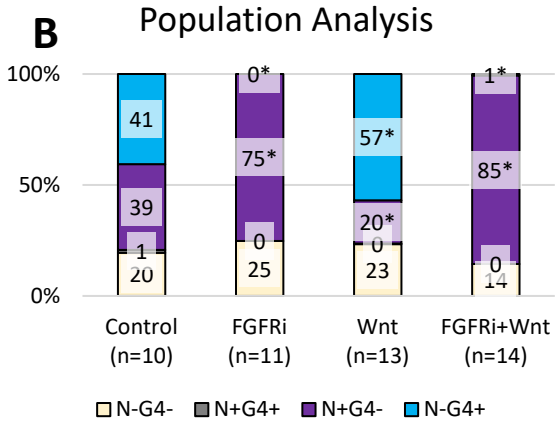

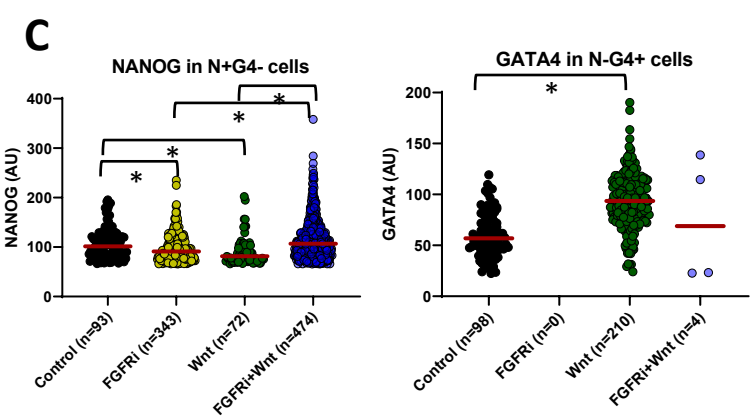

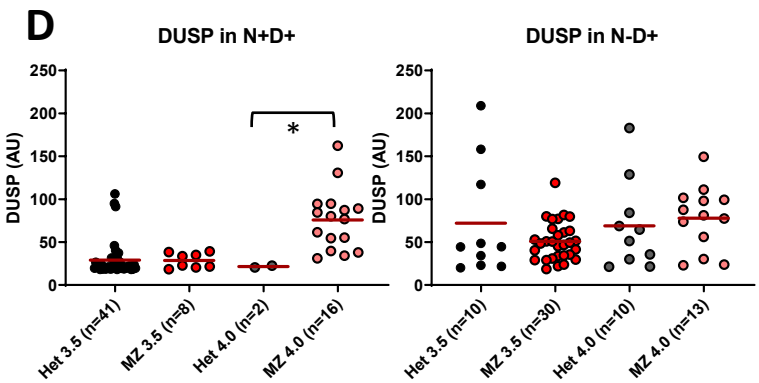

Figure S10: Single cell expression analyses of relevant genes

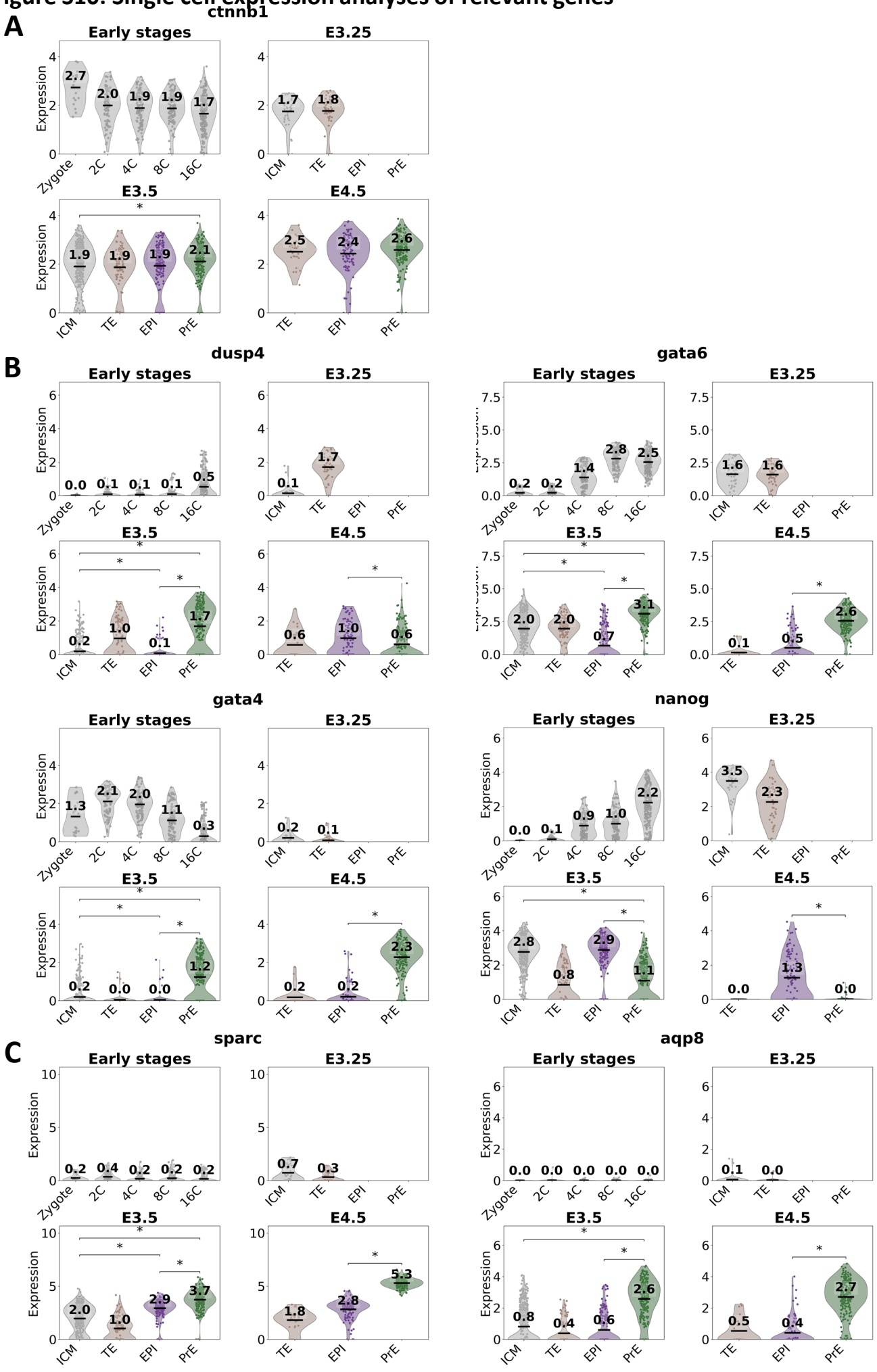

Figure S11: β-catenin absence accelerates GATA6 and GATA4 turnover